Offset Between Surface Elevation Table and Sediment Core Derived Accretion Rates: Case Study from Piermont Marsh, New York

Clara Chang[1*], Sarah Fernald[2], Timothy Kenna[1], Christopher Mitchell[2], Christina Pacella[2], Margie Turrin[1], Jonathan Nichols,[1] Steven Chillrud[1], Dorothy Peteet[1,3]
[1]*Lamont Doherty Earth Observatory of Columbia University, Palisades, NY, 10968, USA*
[2]*Hudson River National Estuarine Research Reserve, Staatsburg, NY, 12580*
[3]*NASA Goddard Institute for Space Studies, New York, NY 10025*
*corresponding author, Clara Chang, cchang@ldeo.columbia.edu, ORCID ID: 0000-0001-7310-639X

Abstract

Surface elevation tables (SETs) are a standard metric for measuring precise sediment accretion in wetlands. They are used to evaluate whether marshes are keeping pace with sea level rise and to determine whether management interventions are needed to prevent marsh inundation. The SET method combined with sediment core studies provides constraints on short-term (annual) and long-term (decadal) accretion rates. Sediment core records provide necessary constraints on slow occurring processes not adequately captured by SET methods such as subsurface decomposition and compaction. This long timescale view is relevant for land management in the context of sea level rise and carbon accumulation. New data are reported from Piermont Marsh, a brackish tidal wetland on the Hudson River. SET measurements reveal accretion rates from 3.1 to 6.5 mm/year from 2019 to 2024, while data from sediment cores collected 2 m from SETs provide rates of 2.4 mm/year and 3.9 mm/year since 1975. The contrast between methods is important for marsh managers interpreting accretion data and understanding the urgency presented by sea level rise for coastal marsh erosion. The relatively high accretion rates measured by SETs imply resilient marshes, but lower long-term rates indicate marshes are in need of assistance to survive. Future research on the North American Atlantic coast tidal wetlands should consider coupling SETs with lead (Pb) abundance measurements on sediment cores using X-Ray Fluorescence Spectroscopy; this is a relatively fast, non-destructive way, (in comparison to radionuclide measurements) to assess accretion rates on decadal timescales, which are needed to accurately estimate marsh resilience to inundation from sea level rise.

Introduction

Coastal wetlands are being lost at increasing rates along the Atlantic Coast of the United States, reflecting a global trend (e.g. Maher and Starke, 2023; Weis et al. 2021; Roman et al. 2023; Haaf et al. 2021; Saintilan et al. 2023; Webb et al. 2013; Fluet-Chouinard et al. 2023). Losses are driven by land use change, pollution, (e.g. Wigand

et al. 2014) and accelerated sea level rise caused by climate change (Valiela et al. 2022). Wetlands provide critical services including water quality maintenance, protection from storms and erosion (Sheng et al., 2021a), carbon sequestration (Barbier et al. 2011) and cultural value (Alikhani et al. 2022).

Sea level rise (SLR) is accelerating on the Atlantic Coast of the United States at 3-4 times faster than the global average (Sallenger Jr et al. 2012) due to ongoing glacial isostatic adjustment (e.g. Peltier, 2004, 2005; Kopp et al. 2014), ice melt (e.g. Gomez et al. 2010; Mitrovica et al. 2009), and changing patterns of ocean circulation (e.g. Yin et al. 2009). Relative sea level rise in the New York City harbor averaged 2.9 mm/yr between 1900 and 1990, increasing to 4.5 mm/yr between 1990 and 2019 (Gornitz et al. 2020). Water levels are rising in Hudson River Estuary marshes at rates consistent with sea level change measured by the tide gauge at the Battery in NYC (Courtney et al. 2023). It is projected that relative sea level (RSL) rise in New York City may be 32% greater than the global average by the end of the century (e.g. Horton et al. 2015; Miller et al. 2013).

Tidal wetlands grow at the land-water interface. As sea level rises, accommodation space is created, which is filled by vegetation growth and sediment deposition (Morris et al. 2002). Slow and moderate rates of sea level rise cause marshes to accrete vertically and horizontally (Morris et al. 2002). Inundation adds mineral sediment and can enhance productivity (Kirwan et al. 2016). Indeed, moderate sea level rise rates over the past ~6,000 years have been responsible for the creation of U.S. Atlantic coast marshes (Peteet et al. 2006; Stevenson et al. 1986; Redfield, 1972). However, if the maximum vertical accretion rate is lower than the rate of relative sea level rise, the marsh will become submerged (Reed, 1995; Kirwan et al. 2010; Fagherazzi et al. 2020). Although some losses may be compensated through migration landward (Kirwan et al. 2016), this is not possible if marshes are blocked by steep slopes (e.g. Molino et al. 2021), human developments (i.e., “coastal squeeze”; Doody, 2004; Valiela et al. 2018; Torio and Chmura, 2013), or starvation of source sediment (e.g. Peteet et al. 2018; Mariotti and Fagherazzi, 2013). Marsh accretion reflects a balance between inputs (e.g., plant growth, sediment deposition) and losses (e.g., erosion, decomposition, dewatering, compaction, and bioturbation), influenced by climate, geology, and human activity (e.g., Cahoon et al. 2015; Holmquist et al. 2021).

Measuring Marsh Accretion

Accurate measurement of sediment accretion is essential to assess whether a marsh is keeping pace with sea level rise (Cahoon et al. 1995; Cahoon, 2015; Webb et al. 2013) and determine if interventions are needed to prevent inundation and wetland collapse (e.g. Raposa et al. 2023). Although a variety of methods have been

employed to evaluate sediment accretion, the main approaches include 1) building high resolution age models from sediment cores and 2) directly measuring the marsh surface with techniques such as marker horizons and surface elevation tables. The two methods are often used interchangeably but can yield significantly different accretion rates from the same marsh, leading to confusion and conflicting guidance for management.

Sediment cores use stratigraphic markers such as lead, copper, zinc, mercury, nitrogen isotopes, and pollen to reconstruct historical accretion tied to pollution and vegetation changes (e.g. Lima et al. 2005; Delaune et al. 1978; Wigand et al. 2014; Brush, 1984; Kearney and Ward, 1986; Chmura et al. 2000). Another key marker is ^{137}Cs, an artificial radionuclide released from nuclear bomb testing (~1950-1980) (Delaune et al. 1978; Faucher et al. 2021). Like other historical markers, ^{137}Cs interpretation can be complicated by additional sources of radioactive contamination (Appleby et al. 1991). In the Hudson River, the ^{137}Cs curve is impacted by historic releases from the Indian Point Nuclear Power Plant and the Knolls Atomic Power Laboratory (Simpson et al. 1976; Bopp et al. 1981). To reduce the dating uncertainty, multi-proxy data approaches are recommended to create a regional historical-marker dataset (e.g. Wright et al. 2017; Kemp et al., 2011, 2017; Peteet et al. 2018, 2020).

In contrast, artificial marker horizons provide direct, short-term surface accretion measurements by installing a reference layer and tracking sediment accumulation above it, however, they do not account for subsurface processes such as belowground growth (Bartholy et al. 2004; Goodman et al. 2007; Lacy et al. 2020). The surface elevation table (SET) method (later developed into the rod surface elevation table marker horizon, RSET-MH system) was designed to directly measure subsurface processes (Figure 1; Schoot and deJong, 1982; Boumans and Day, 1993; Cahoon et al. 1995; Cahoon et al. 2002a; Cahoon et al. 2002b; Cahoon et al. 2015). In this method, a rod is driven up to 40 m into the substrate and fitted with a leveled arm with eight fixed positions. Surface elevation is determined by lowering pins in the SET arm to the wetland surface and measuring the height of each pin relative to the arm at each fixed position. The distances between the arm and the wetland surface provide a measure of wetland elevation change (Cahoon et al. 2015). Elevation change is often compared to an artificial marker horizon (MH) -typically feldspar clay- monitoring plot, which is used to calculate “shallow subsidence” processes of compaction and decomposition. Measurements are typically collected every three months (Lynch et al. 2015).

Comparing SET and Long-Term Accretion Rates

A compilation of SET and sediment core accretion rates from coastal wetlands around the world shows a significant offset between the two methods (Breithaupt et al. 2018). If the SET study is not corrected with a marker

horizon, the offset includes shallow subsidence (Cahoon et al. 2015). Differences can also be attributed to timescale; cores typically capture much longer periods of accretion than SETs. The shorter timescale represented in SET records is less likely to capture periods of non-deposition and erosion, as well as longer term processes of compaction and organic matter decomposition (Wiberg et al. 2020; Sadler, 1981; Sommerfield, 2006). Conversely, sediment cores may also capture events that add a significant amount of sediment deposition to a system, such as flooding and storms (Callaway, 1996; Tweel & Turner, 2014). However, sediment core and marker horizon studies can also be impacted by bioturbation and other processes that mix sediments and disturb stratigraphy (e.g. Swales and Lovelock, 2020) though, modeling can correct for these processes (Olsen et al. 1978).

Offsets are also explained by temporally variable SLR trends; it is difficult to directly compare accretion rates averaged over different lengths and periods of time. In the northeastern United States, RSLR (relative sea level rise) has been spatially and temporally variable due to glacial isostatic adjustment and regional factors including groundwater withdrawal and compaction (Kemp et al. 2011, 2017; Miller et al. 2013; Peltier, 2006, Rovere et al. 2016; Englehart & Horton, 2012). For example, according to a sediment core-derived record from foraminifera and $\delta^{13}C$ in a New York City tidal wetland, relative sea level rise (RSLR) has varied from 0.5 mm/year in 600-1000 CE to 1.52 mm/year at 1400 CE. Around 1630 CE, RSLR was 1.37 mm/year; this rate steadily rose to 2.98 mm/year in 2014 consistent with tide gauge data (Kemp et al. 2017).

The timescale question has been central to ongoing studies estimating global wetland vulnerabilities and local wetland management with respect to RSLR (Wiberg et al. 2020). On one hand, it has been argued that it is inappropriate to use slower, millennial scale SLR scenarios while the current rate of sea level change is so much higher than historical values; in this argument shorter term SET derived data should hold greater weight (e.g. Kirwan et al. 2017). On the other hand, longer timescale processes such as compaction, decomposition, and singular events of erosion, deposition, and non-deposition have a major effect on vertical accretion and must be considered (e.g. Parkinson et al. 2017). Recent studies show that a 50-year RSL trend is the best predictor of tidal wetland resilience to inundation (Saintilan et al. 2022; Hein et al. 2024). Formal analyses reconciling SET records and longer-term core derived measurements are needed to understand factors influencing small scale local variability (Breithaupt et al. 2018; Wiberg et al. 2020). Specific protocols must be developed to inform interpretation of individual data sets for research and management.

There are few studies on long-term accretion rates comparing cores and nearby SET monitoring locations. Breithaupt et al. (2018) identified case studies from the northeastern and southwestern United States. They found a large degree of spatial variability and few correlations to quantify the relationship between the two methods. Hein et al. (2024) attempted to extrapolate 50-year accretion rates from SET data in the Georgia Bight, but found these rates to be overly high compared to relative sea level curves and sediment cores. We conducted an updated literature review on mid-Atlantic sites with both core and SET data, finding a similar absence of overlapping records (Table 1). SET rates are generally higher; however, they are more comparable to sediment core data in longer SET monitoring studies (Table 1). No clear trends emerged that could easily reconcile these two methods. More detailed side-by-side comparisons of SETs and cores are needed (Breithaupt et al., 2018). These comparisons must be paired with context on local hydrologic processes, nutrients, vegetation, and long-term land use and environmental trends.

To address this research gap, we collected two 1-meter-long sediment cores next to (~2 meters away) SET stations in Piermont Marsh, Piermont, NY. We measured historic pollution chronologies using X-Ray Fluorescence Spectroscopy (XRF), a rapid, non-destructive method of determining the elemental composition of sediment (Kenna et al. 2011). By using a lead pollution chronology, we calculate the 50-year accretion rate needed to predict marsh resilience (Saintilan et al. 2022) and compare with SET data. By comparing SET and sediment core data, we provide constraints on longer-timescale processes causing vertical decrease in sediment elevation such as compaction, decomposition and depositional hiatuses. We employ loss on ignition (LOI), potassium, and titanium measurements, and nitrogen stable isotopes to evaluate sediment stability and mineral input.

Methods

Study Site: Piermont Marsh

Piermont Marsh is a brackish tidal wetland (salinity ranges from 0-12 ppt, NYSDEC 2019) on the western side of the Hudson River estuary. It is a federally protected Hudson River National Estuarine Research Reserve (HRNERR) site. It is bracketed to the north by Piermont Pier and to the west by Tallman Mountain State Park, which includes the 100 m vertical Palisades Sill.

Sediment accretion in this marsh is a function of the integrated tidal and hydrological systems. Piermont Marsh is connected to Sparkill Creek and the Hudson River. Permanent, shallow tidal creeks traverse the marsh. Sparkill Creek drains 11.1 square miles of a predominantly urban watershed and discharges into the north end of the marsh (NYSDEC 2019). In 2021, water testing showed high turbidity, high nutrients, and chlorophyll a

concentration (Riverkeeper, 2022). To the best of our knowledge, the sediment load and composition for Sparkill Creek has not been characterized. The Hudson River estuary is a 38,000 km^2 watershed. It is microtidal, with an average tidal range of 1.5 m (Ralston et al. 2020a) and freshwater input is highly seasonal (Olsen et al. 1978). The largest tributaries in terms of both water discharge and sediment load are the Upper Hudson and Mohawk River (Wall et al. 2008). However, smaller tributaries are also a significant sediment source (Nitsche and Kenna, 2018). The total estimated sediment load for the estuary is 1.2 Mt/year (Ralston et al. 2020b).

Piermont Marsh is significant in terms of age and depth compared to nearby marshes. At 13.7 m peat depth, it has a radiocarbon (^{14}C) age of 5,700 before present (Peteet et al. 2006). The 1,030-acre wetland represents a major reservoir for carbon storage (Peteet et al. 2020). Its sedimentary dynamics are a function of the integrated history of surrounding land use. Piermont Marsh and the adjacent territory are the ancestral homeland of the Tappan tribe of the Lenape people (Baker et al. 2022). Pollen records indicate this region was colonized by European settlement in the 1700s (Pederson et al. 2005). Settlement is evident from a decline in tree pollen and increase in *Ambrosia* (weedy ragweed) typical of forest clearance and subsequent mineral sediment input due to enhanced erosion (Pederson et al. 2005). The paleo-ecological record shows that the 20th century brought reforestation (Pederson et al. 2005) and large population growth. This change is reflected in measurements of industrial metal and nitrogen pollution (Peteet et al. 2020). Half a century ago, Piermont Marsh was covered by 66% *Spartina patens* and *Distichlis spicata* (saltmarsh hay and saltgrass; native marsh grasses) as well as *Typha angustifolia* (narrowleaf cattail; invasive) (Peteet et al. 2020). Today, the landscape is almost entirely dominated by invasive *Phragmites australis* (common reed), with small patches of native vegetation.

Study Site: Sea Level Rise Resilience

Several studies have investigated and modeled the resilience of Piermont Marsh and nearby tidal wetland systems to sea level rise. Tabak et al. (2016) used the Sea Level Affecting Marshes Model (SLAMM) to simulate changes in the Hudson River estuary by the year 2100 under medium (88 cm SLR by the year 2100) and high sea level rise scenarios (187 cm SLR by the year 2100). They modeled these two scenarios using low (maximum 5 mm/year), medium (maximum 10 mm/year) and high accretion rates (maximum 15 mm/year). Modeling shows that with medium SLR and high accretion, Piermont Marsh would largely stay high marsh. With medium SLR and low accretion, Piermont would be converted to almost entirely low marsh. With high SLR, high accretion, Piermont

would be converted largely to tidal flats. If there was high SLR and low accretion, Piermont Marsh would be completely drowned by estuarine water in the next 80 years (Tabak et al. 2016).

Various rates have been cited for Piermont Marsh and nearby brackish Hudson River tidal wetlands. Peteet et al. (2020) found that accretion rates in Piermont Marsh range from 1 to 6 mm/year over 2000 years, with an average of 2 mm/year. This finding is consistent with a synthesis of ^{137}Cs based accretion rates from the Atlantic Coast that shows natural marshes have an upper limit of 5 mm/year accretion (Holmquist et al. 2021). Feldspar marker horizons show a 7 mm/year accretion rate from 2013 to 2015 (Dubossi et al. 2015). Sheng et al., (2021b) suggest that Piermont Marsh accretion may be closer to 10 mm/year. They contend that *Phragmites australis,* the dominant vegetation in Piermont, increases accretion rates. Sheng et al. (2021b) based this rate on SET measurements from *Phragmites* dominated areas in Chesapeake Bay (Rooth & Stevenson, 2000) and New Jersey (Weis et al. 2021). Piermont Marsh is already showing signs of increased inundation. In 2019, relative to 1999, the surface flooded more frequently (Courtney et al. 2023; Montalto et al. 2006).

Coring and Sampling

Cores were collected using a side-opening Russian Dachnowski corer approximately 2 m from SET sites 2 and 4 (Figure 2, cores PMT 2 and PMT 4). PMT 2 is further from the Hudson River estuary, and is 30 m away from the stream (Figure 2C). PMT 4 is closer to the Hudson River estuary (Figure 2D). Both cores were collected in areas completely dominated by *Phragmites*. The side-opening corer design was used to avoid compaction artifacts (Belokopytov and Beresnevich 1955; Jowsey, 1966; Faegri and Iversen 1975; Smeaton et al. 2020). Cores were wrapped in plastic wrap and aluminum foil, labeled, and refrigerated at the Lamont Doherty Earth Observatory core repository.

The sediment cores were sampled, dried in a 50°C oven overnight, and homogenized with a mortar and pestle. Samples of carbon and nitrogen stable isotopes and for carbon and nitrogen concentrations were measured by the Cornell University Stable Isotope Laboratory (COIL) on a Thermo Delta V isotope ratio mass spectrometer (IRMS) interfaced to a NC2500 elemental analyzer. Loss on ignition (LOI) samples were incinerated at 550°C for two hours in a combustion furnace (Dean, 1974). Samples were measured for ^{137}Cs and other gamma emitting radionuclides in sealed tubes in a low-background, intrinsic germanium well detector. XRF elemental chemistry measurements were conducted on the split sediment core by the ITRAX core scanner at Lamont Doherty Earth Observatory core repository (30kV, 55mA, 10 seconds, 0.5cm step size; Cox Analytical Systems). XRF

measurements were not calibrated with external chemistry because relative elemental abundance, rather than absolute concentrations, were important to this study.

Hierarchical cluster analysis was used to identify the lead rise and subsequent decline to calculate accretion rates (hclust function, stats package; R Core Team, 2013). The rise has been dated to between 1830-1850 with AMS radiocarbon dates and pollen analysis in Piermont Marsh (Pederson et al. 2005; Peteet et al. 2020) as well as ^{210}Pb near the Great Lakes (Edgington and Robbins, 1976; Farmer, 1978; Yohn et al. 2004). In this paper we use 1839 as a date for lead rise consistent with Pb isotopes in Jamaica Bay Marsh (Peteet et al. 2018). The decline in lead concentration has been previously demonstrated to be 1975 in the Hudson River via ^{210}Pb and ^{137}Cs of Hudson River estuary (Nitsche et al., 2010) and nearby tidal wetlands (Sritrairat et al. 2012). In the northeastern United States, the lead rise is associated with industrial revolution coal burning and the fall is associated with the phase-out of leaded gasoline (e.g. Yohn et al. 2004) or municipal solid waste incineration in New York City (Chillrud et al. 2004). We estimate accretion by dividing how much sediment accumulated since 1850 and 1975 respectively, by the numbers of years represented; the top of the core is the year the core was collected (e.g. 2020-1839 = 181 years; 2020-1975 = 45 years).

SETs

SETs were installed in 2019, following protocols from Lynch et al. (2015). These areas were dominated by *Phragmites* throughout the study period. Rods were installed to refusal at depths between 18 m and 23 m with a gasoline powered jackhammer. A sectional platform was installed around each SET to ensure monitoring activities did not cause subsidence, or surface disturbance. Elevation change was measured seasonally (except during winter months). Surface disturbance, such as ice, footprints (from animals such as deer, raccoons), burrows, and other animal activity were noted and interactions with pin locations were flagged with data codes. The SET record discussed in this paper spans from May 2019 to October 2023.

Results

Lead Curve

Core PMT 2 shows a Pb rise at 41 cm and decline at 11.5 cm (Figure 3, Table 2). Core PMT 4 shows a Pb rise at 56 cm, and decline at 18.5 cm. The PMT 2 core has a pronounced, narrow lead peak (Figure 3, Table 3).

Carbon and Nitrogen Stable Isotopes and Concentrations

Nitrogen concentration (%N) is between 1-2% through cores PMT 2 and PMT 4. $\delta^{15}N$ values increase after 1839 in both cores. Carbon concentration (%) is variable throughout both cores and has a range from 10% to 44% (Figure 4, Figure 5), shows a decline from about 70 to 40 cm, increases again to about 1975, and then declines towards the top of the core. Carbon concentration is correlated with LOI (Figure 6). Titanium and potassium are highly correlated with one another (Figure 6) and negatively correlated with LOI (Figure 6).

Accretion Rates from Piermont Cores and SETs

The accretion rate measured from RSET 2 is 5.2 mm/year (Table 6), while the core collected 2 m away shows an accretion rate of 3.91 mm/year (Table 7, Figure 7). The accretion rate measured from RSET 4 is 5.6 mm/year (Table 6), while the core collected 2 m away shows an accretion rate of 2.43 mm/year (Table 7). The core collected in the north of Piermont Marsh (sampled in the year 2000) shows an accretion rate of 1.72 mm/year (Table 7). The core collected in the south of Piermont Marsh, also sampled in the year 2000 and dated with ^{137}Cs, yields an accretion rate of 3.70 mm/year (Table 7). The average accretion rates calculated from sediment cores is 2.94 mm/year (Table 7). Accretion rates calculated from RSETs collected in the entire east-west transect range from 3.1 to 6.5 mm/year with an average of 4.97 mm/year (Table 6). We also calculated accretion rates based on the lead rise in 1850. The 1850-2020 average accretion rate for core PMT 2 was 2.44 mm/year, in contrast to the 1975-2020 average accretion rate for PMT 2 which was 3.91 mm/year (Table 7). The 1850-2020 average accretion rate for core PMT 4 was 3.05 mm/year, in contrast to the 1975-2020 average accretion rate for PMT 4 which was 2.43 mm/year (Table 7).

Discussion

Sea Level Rise Resilience in Piermont Marsh

The 50-year average accretion rates calculated from sediment cores PMT 2 and PMT 4 (2.43 mm/year and 3.91 mm/year) are close to local sea level rise (3.69 mm/year at the Battery in 2022), indicating that the marsh is in danger of inundation with SLR (Saintilan et al. 2022). Two additional cores collected in 2000 show accretion rates of 1.72 mm/year (1975-2000, Peteet et al. 2020) and 3.70 mm/year (1963-2000, this study), which also show lower accretion rates of concern to the future of the wetland. The lowest SET measurement (3.1 mm/year) is also lower than SLR, however, other SET measurements are slightly higher (4.5-6.5 mm/year). These rates are all lower than

the 10 mm/year accretion predicted for Piermont Marsh to keep up with severe SLR scenarios over the next 80 years (Tabak et al. 2016, Sheng et al. 2022).

Accretion rates appear to be increasing over recent years. The 1975-2020 average accretion rates calculated from cores are higher than the 1975-2000 average accretion rates calculated from cores (Table 7). Since these two numbers are averaged over different periods of time, the 1975-2020 accretion rates should include a greater signal of compression and decomposition. Therefore, it appears likely that accretion rates are truly increasing. This trend is consistent with rising sea levels and increasing accommodation space (Kirwan et al. 2016). Since the cores collected in 2000 were collected in different parts of Piermont Marsh, this observation may also be a reflection of local vegetation, and topography. For the PMT 2 core, higher accretion rates may also be due to proximity to a nearby stream. Higher soil drainage increases aeration and results in higher productivity (Chmura and Hung, 2004). This is supported by the finding that PMT 2 has a higher average carbon content than PMT 4 (Figures 3, 4).

The very recent higher rates of accretion may also be due to enhanced productivity from nitrogen fertilization (e.g. Martina et al. 2016). Nitrogen concentrations in surface sediment collected in 2020 (1.16% and 1.92%) are higher than nitrogen concentration in 2000 (1.00%) (Table 8). Enriched $\delta^{15}N$ values near the top of the core are consistent with wastewater and fertilizer pollution. This phenomenon is occurring in other systems such as Jamaica Bay (Wigand et al. 2014; Peteet et al. 2018) and Long Island Sound (Copple et al. 2022). It is also possible that accretion rates are supported by higher sediment discharge in the Hudson River since the extreme precipitation and flooding in 2011; this observation is supported by rising inorganic sediment inputs (Ralston et al. 2020a). Mineral sediment influx is also likely influenced by construction of the Mario Cuomo Bridge from 2013-2018 (Berger, 2017). Increased sediment load may also be a result of dam removal efforts in the Hudson River estuary (Wu et al. 2017; Wu and Knack, 2015; Tonitto and Riha, 2016); even if this sediment flux represents a small proportion of overall estuary discharge (Ralston et al. 2021). Finally, it is also possible that the increasing density of *Phragmites* may be impacting accretion rates. Interestingly, the 1850-2020 average accretion rates are generally comparable to the 1975-2020 accretion rates in spite of many changing factors in land use, vegetation, and hydrology (Table 7).

Our findings about Piermont Marsh's vulnerability to submergence from SLR are particularly significant because this marsh closely flanks the Village of Piermont. Modeling analysis shows that this marsh buffers the nearby community from waves, floods, and structural loss during storms. During Superstorm Sandy in 2013,

Piermont Marsh reduced flooding by 8% and wave activity by 11% (Sheng et al. 2021). As sea levels rise, the marsh will also be an important buffer against smaller floods and wave action (Sheng et al. 2022). Degradation of this marsh also raises concerns about the release of anthropogenic organic compounds (e.g. Mittal and Rockne, 2010) and heavy metals (Figure 3, Peteet et al. 2020) into the surrounding tidal waters, which have toxic health risks. Further loss of habitat would also impact native and migratory species that rely on this fundamental wetland habitat (e.g. Wells et al. 2008) and their critical roles in the food web.

Shallow Subsidence

Piermont Marsh is a difficult site to monitor because the vegetation is almost entirely dominated by invasive *Phragmites australis*. *Phragmites'* fibrous roots make it difficult to use the feldspar artificial marker horizon method. In Piermont Marsh, the feldspar layer degrades after ~5-10 years. Therefore, the artificial marker horizon method cannot capture decadal-scale subsurface processes important to vertical accretion. Here, we use the historic lead pollution prevalent throughout the northeastern United States (and likely elsewhere) to provide an independent, 50-year timescale estimate of sediment accretion which captures signals of decomposition and compaction ("shallow subsidence", Figure 1).

The offset between sediment cores (1.72-3.91 mm/year) and SETs (3.1-6.5 mm/year) represents 50-years of marsh surface decrease, including dewatering, compaction, bioturbation, decomposition, and singular events of erosion and non-deposition. Variable LOI, bulk density, macrofossil assemblages, $\delta^{13}C$ and $\delta^{15}N$ (Peteet et al. 2020) show that sediment composition changes significantly down the core. This is because different materials are undergoing diagenesis at varying timescales. The 50-year accretion period may also include hiatuses from both stream dynamics (Figure 3) and from historical changes in climate and vegetation. During the intense human impact interval (80-40 cm), for example, deforestation led to increased mineral input into the marsh and changed sedimentation rates (Peteet et al. 2020). There may also be a bioturbation effect. Oligochaete and polychaete worms were found in the upper 10 cm in Piermont Marsh sediments (Mittal and Rockne, 2010). Notably, *Nereis* found in Piermont substrate were 20-30 mm long, and *Hobsonia florida* were 7-15 mm long. These animals are large enough to alter sediment geometry and change drainage patterns (Mittal and Rockne, 2010). However, worms are more likely to be present in the ponds. We have never observed macroinvertebrates of any kind in peat sediment cores and given the consistent stratigraphy in palynology, isotopes, and dating amongst several cores sampled throughout the marsh platform, it is unlikely that bioturbation is mixing very large amounts of sediment. Fiddler crabs are also

present; however, they predominantly stay on the marsh edges and do not appear to burrow into the dense *Phragmites* platform.

Another potential factor in shallow subsidence is decomposition: in tidal wetlands, processes include oxidation, methanogenesis, denitrification, and sulfate reduction (Stevenson et al. 1986). A higher water table and the presence of *Phragmites australis* may increase methanogenesis (Grunfeld and Brix, 1999). Higher salinity may decrease denitrification (Osborne et al. 2015). Extended tidal reach and hydroperiod (Courtney et al. 2023) could change marsh drainage pathways, potentially increasing sediment flushing, and release of nutrients into the estuary (Wilson and Morris, 2012). Enhanced inundation could potentially reactivate dormant microbial communities and organic decomposition at depth (Steinmuller et al. 2019, Steinmuller and Chambers, 2019, Vaughn et al. 2020). Such decomposition processes are likely significant, as there is high lateral carbon export flux from tidal wetlands to estuaries in eastern North America (Najjar et al. 2018).

Deep Subsidence

Vertical movement occurring below the SET rod is termed "deep subsidence" (Figure 1, Cahoon et al. 2015). For example, it is known that glacial isostatic adjustment (GIA) is causing subsidence on the Atlantic Coast at ~2 mm/year (Davis and Mitrovica, 1996). GIA is captured in RSLR measurements at the Battery and therefore included in our sea level resilience assessment. However, there may be other local subsidence effects that would not be captured by the Battery tide gauge and have an impact on wetland elevation with respect to sea level (Hammond et al. 2021). For example, Piermont Marsh and nearby marshes are unique because they are underlain by a very thick layer of sediment. Seismic refraction and borehole data ~5 miles north of Piermont in the Hudson River estuary show 255 m of sediment overlaying the local Triassic age bedrock. The top 30 m of sediments are organic rich silt (Worzel and Drake, 1959; Herron et al. 1968). Piermont SETs are installed ~15 m into sediments; it was not feasible to install into bedrock (Figure 1). Therefore, it is possible that the SETs, and indeed the whole marsh, are subject to long-timescale, slow subsidence, although practical implications are unclear. It has also been hypothesized that Hudson River tidal wetlands could be influenced by the Ramapo Fault Zone (RFZ); graben-like downfaulting could potentially cause local subsidence (Newman et al. 1987). Numerous earthquakes over the past century have been attributed to movement by the Ramapo Fault and nearby secondary faults (Page et al. 1968), including a magnitude 4.8 earthquake on April 5, 2024, with an epicenter near Lebanon, NJ (USGS, 2024). The signal in local subsidence from neo-tectonics is supported by the exceptional age and depth of Piermont Marsh. Piermont Marsh

peat depth relative to other tidal wetlands suggests subsidence resulting in increased accommodation space over several millennia. We recommend more research on this topic in the form of geophysical surveys and characterization of the subsurface marsh structure.

Importance of Old Wetlands

It has been suggested that globally (Kirwan et al. 2016) and in the Hudson River estuary system (Tabak et al. 2016; Yellen et al. 2020), new marshes will form to compensate for the loss of old marshes, causing little net loss with sea level rise. For example, shallow new marshes are rapidly accreting in the Hudson River estuary behind railroad berms, jetties and dredge spoil islands (Yellen et al. 2020). These marshes are primarily clastic material and have very low LOI values (Yellen et al. 2020). In contrast, Piermont Marsh, which is over 13 m deep, represents over 6000 years of carbon storage (Peteet et al. 2006) and has significantly higher organic carbon content. Restored English marshes show that it takes at least 100 years for new wetlands to store the same amount of carbon as natural wetlands yearly (Alongi et al. 2022; Burden et al. 2019; Drexler et al. 2019). Wetlands formed over the past 3,000-4,000 years or more store significantly more carbon globally than newer regions (Rogers et al. 2019; Saintilan et al. 2022). It is therefore critically important to protect these deep marshes.

Cores Measure Long Timescale Accretion Processes

The main arguments for RSET-MH monitoring (opposed to sediment cores) are that they do not require as much historical land use information as a sediment core study, and can be easily integrated in global monitoring networks (Mackenzie et al., 2023; Webb et al., 2013; Bansal et al., 2023). However, monitoring RSET-MH systems requires a significant amount of fieldwork. It takes several years to generate usable data (Lynch et al., 2015). Feldspar markers from artificial marker horizons can degrade and be difficult to monitor in *Phragmites* dominated sites. Previous papers have stated that core-based studies require specialized coring equipment, and associated analyses and chemistry require time, and expertise (Mackenzie et al., 2023). The vast majority of core-based sediment studies exclusively use ^{137}Cs and ^{210}Pb to calculate accretion rates to estimate wetland response to SLR.

Using the methods outlined in this study, core data can be generated and analyzed relatively quickly; accretion rates can be calculated in a matter of days, rather than years. We use lead pollution from the industrial revolution to calculate a 50-year accretion rate recommended by Saintilan et al (2022) to be the best predictor of marsh resilience with sea level rise. Lead was measured in sediment cores with X-Ray fluorescence spectroscopy (XRF) using an ITRAX core scanner (Croudace and Rothwell, 2015), which rapidly assesses elemental composition

down-core in hours. The benefit of scanning XRF is that it can provide sub-millimeter (60 μm) resolution down-core in hours, with little to no sediment core preparation or pre-treatment (Cox Analytical Systems). Samples can also be dried, homogenized, and measured on handheld XRF compared against standard reference materials, which provides quantitative elemental concentrations (Kenna et al. 2011). Moreover, a full suite of historical elemental data provides significant context on the depositional environment. For example, potassium and titanium are highly correlated with inorganic matter, indicating that these are very good elemental proxies for upland weathering and clay input (Figures 3,4,5). Other lithogenic elemental ratios may be useful to assess mineralogical change and sediment provenance (Nitsche and Kenna, 2018; Figures 3, 4, 5). This study also provides additional support for using LOI to estimate carbon concentration in brackish tidal wetland sediments. Carbon content (%) and LOI are highly correlated, indicating that LOI is an effective method to estimate wetland carbon concentration (Figure 5, e.g. Maxwell et al. 2023).

The XRF-generated lead stratigraphy approach towards measuring accretion could be widely adopted in the United States and other well studied, urban regions because lead deposition from industrialization is well dated in sedimentary records. In the northeastern United States, the 1975 decline in atmospheric lead deposition has been seen in sediment cores from rivers, marshes and lakes from New York, New Jersey, and Connecticut (e.g. Bopp et al. 1993; Wenning et al. 1994; Benoit et al. 1999a, 1999b; Chillrud et al. 1999, 2003; Weis et al. 2005; Lima et al. 2005; Nitsche et al., 2010; Sritrairat et al., 2012, 2013; Peteet et al., 2018, 2020; Copple et al., 2023). Similar lead curves are seen in the Great Lakes (rise in 1850, fall in 1975; e.g. Edgington and Robbins, 1976; Farmer, 1978; Graney et al. 1995; Yohn et al. 2004), and from 47 ^{210}Pb-dated sediment cores from the Adirondacks, Vermont, and Nova Scotia (Dunnington et al. 2020). It is important to exercise caution, as local contamination can impact lead chronology. Therefore, we recommend that reference cores be collected at specific sites first, and tools such as ^{137}Cs, ^{210}Pb, ^{14}C, and palynology be used to establish age chronology. Detailed historical research on different sources of contamination should be conducted to understand the environmental and geological systems impacting sediment composition. Historical markers such as lead concentration can be identified and used in accretion monitoring studies.

Conclusion

Based on sediment core data, the 50-year accretion rate for Piermont Marsh is ~3 mm/year. This finding indicates that the marsh is at risk from inundation due to sea level rise in the next 80 years as defined by the medium and high

SLR scenarios proposed by Tabak et al. (2016). The offset between sediment cores (1.72-3.91 mm/year) and SETs (3.1-6.5 mm/year) represents 50 years of marsh surface vertical decrease, including dewatering, compaction, bioturbation, decomposition, and events of erosion and non-deposition. Degradation of Piermont Marsh would represent a significant loss of stored carbon, which will not be easily offset by new marshes forming in anthropogenic backwaters and in upland areas. Scanning X-Ray Fluorescence Spectroscopy (XRF) in sediment cores is a rapid way to estimate historical pollution markers in the northeastern United States to calculate 50-year accretion rates relevant to assessing marsh resilience to SLR.

Declarations

Ethics approval and consent to participate

Not applicable

Consent for publication

Not applicable

Availability of data and materials

All data generated or analysed during this study are included in this published article and in the supplementary information.

Competing interests

The authors declare that they have no competing interests

Funding

Support from the Margaret A Davidson Fellowship.

Author's Contributions

Clara Chang led the study and is the primary author of the manuscript. Laboratory analyses were conducted by Clara Chang, Dorothy Peteet and Steven Chillrud. Clara Chang, Sarah Fernald, and Dorothy Peteet collected the core samples. Sarah Fernald, Christopher Mitchell, Christina Pacella collected SET data. Timothy Kenna and Jonathan Nichols assisted with data interpretation and analysis. Margie Turrin provided site specific information. All authors assisted with interpreting the data and writing the manuscript.

Acknowledgements

Not applicable

References

Alongi, D. M. (2023). Current status and emerging perspectives of coastal blue carbon ecosystems. *Carbon Footprints*. Vol. 2, Issue 3. https://doi.org/10.20517/cf.2023.04

Alikhani, S., Nummi, P., & Ojala, A. (2021). Urban Wetlands: A Review on Ecological and Cultural Values. *Water*. Vol. 13, Issue 22, p. 3301. https://doi.org/10.3390/w13223301

Appleby, P. G., & Oldfield, F. (1978). The calculation of lead-210 dates assuming a constant rate of supply of unsupported 210Pb to the sediment. *Catena.* Vol. 5, Issue 1, pp. 1–8. https://doi.org/10.1016/s0341-8162(78)80002-2

Armentano, T. V., & Woodwell, G. M. (1975). Sedimentation rates in a Long Island marsh determined by 210Pb dating. *Limnology and Oceanography.* Vol. 20, Issue 3, pp. 452–456. https://doi.org/10.4319/lo.1975.20.3.0452

Artigas, F., Shin, J. Y., Hobble, C., Marti-Donati, A., Schäfer, K. V. R., & Pechmann, I. (2015). Long term carbon storage potential and CO2 sink strength of a restored salt marsh in New Jersey. *Agricultural and Forest Meteorology.* Vol. 200, pp. 313–321. https://doi.org/10.1016/j.agrformet.2014.09.012

Artigas, F. J., Grzyb, J., & Yao, Y. (2021). Sea level rise and marsh surface elevation change in he Meadowlands of New Jersey. *Wetlands Ecology and Management.* Vol. 29, Issue 2, pp. 181–192. https://doi.org/10.1007/s11273-020-09777-2

Baker, J., Coumans, H., and Whitney, J. Lenapehoking: An Anthology.

Bansal, S., Creed, I. F., Tangen, B. A., Bridgham, S. D., Desai, A. R., Krauss, K. W., Neubauer, S. C., Noe, G. B., Rosenberry, D. O., Trettin, C., Wickland, K. P., Allen, S. T., Arias-Ortiz, A., Armitage, A. R., Baldocchi, D., Banerjee, K., Bastviken, D., Berg, P., Bogard, M. J., … Zhu, X. (2023). Practical Guide to Measuring Wetland Carbon Pools and Fluxes. *Wetlands.* Vol. 43, Issue 8. https://doi.org/10.1007/s13157-023-01722-2

Bartholdy, J., Christiansen, C., Kunzendorf, H. (2004) Long term variations in backbarrier salt marsh deposition on the Skallingen peninsula – The Danish Wadden Sea. *Marine Geology.* 203, 1–2. https://doi.org/10.1016/S0025-3227(03)00337-2

Barbier, E. B., Hacker, S. D., Kennedy, C., Koch, E. W., Stier, A. C., & Silliman, B. R. (2011). The value of estuarine and coastal ecosystem services. *Ecological Monographs.* Vol. 81, Issue 2, pp. 169–193. https://doi.org/10.1890/10-1510.1

Bartholdy, J., Pedersen, J. B. T., & Bartholdy, A. T. (2010). Autocompaction of shallow silty salt marsh clay. *Sedimentary Geology.* Vol. 223, Issues 3–4, pp. 310–319. https://doi.org/10.1016/j.sedgeo.2009.11.016

Belokopytov, I.E. & Beresnevich, V.V. (1955) Giktorf's peat borers. *Torfyanaya Promyshlennost,* 8, 9–10.

Benoit, G., Rozan, T. F., Patton, P. C., & Arnold, C. L. (1999a). Trace Metals and Radionuclides Reveal Sediment Sources and Accumulation Rates in Jordan Cove, Connecticut. *Estuaries.* Vol. 22, Issue 1, p. 65. https://doi.org/10.2307/1352928

Benoit, G., Wang, E. X., Nieder, W. C., Levandowsky, M., & Breslin, V. T. (1999b). Sources and History of Heavy Metal Contamination and Sediment Deposition in Tivoli South Bay, Hudson River, New York. *Estuaries.* Vol. 22, Issue 2, p. 167. https://doi.org/10.2307/1352974

Berger J. (2017) Bridge of Brand Ambitions Is Set to Open at the Tappan Zee. New York Times. 2017/08/24. https://www.nytimes.com/2017/08/24/nyregion/tappan-zee-bridge-opening.html

Binford, M. W.: (1990) Calculation and uncertainty analysis of 210Pb dates for PIRLA project lake sediment cores. J. Paleolimnol., 3, 253–267, https://doi.org/10.1007/BF00219461

Bopp, R. F., Simpson, H. J., Olsen, C. R., & Kostyk, N. (1981). Polychlorinated biphenyls in sediments of the tidal Hudson River, New York. *Environmental Science & Technology*, *15*(2), 210-216. https://doi.org/10.1021/es00084a007

Bopp, R. F., Simpson, H. J., Olsen, C. R., Trier, R. M., and Kostyk, N. (1982) Chlorinated hydrocarbons and radionuclide chronologies in sediments of the Hudson River and estuary, New York, Environ. Sci. Technol., 16, 666–676, https://doi.org/10.1021/es00104a008

Bopp, R. F., Simpson, H. J., Chillrud, S. N., & Robinson, D. W. (1993). Sediment-Derived Chronologies of Persistent Contaminants in Jamaica Bay, New York. *Estuaries.* Vol. 16, Issue 3, p. 608. https://doi.org/10.2307/1352798

Boumans, R. and J. W. Day, Jr. 1993. High precision measurements of sediment elevation in shallow coastal areas using a sedimentation-erosion table. *Estuaries* 16:375-380.

Burden, A., Garbutt, A., & Evans, C. D. (2019). Effect of restoration on saltmarsh carbon accumulation in Eastern England. *Biology Letters.* Vol. 15, Issue 1. https://doi.org/10.1098/rsbl.2018.0773

Breithaupt, J. L., Smoak, J. M., Smith, T. J., III, & Sanders, C. J. (2014). Temporal variability of carbon and nutrient burial, sediment accretion, and mass accumulation over the past century in a carbonate platform mangrove forest of the Florida Everglades. *Journal of Geophysical Research: Biogeosciences.* Vol. 119, Issue 10, pp. 2032–2048. https://doi.org/10.1002/2014jg002715

Breithaupt, J. L., Smoak, J. M., Byrne, R. H., Waters, M. N., Moyer, R. P., & Sanders, C. J. (2018). Avoiding

timescale bias in assessments of coastal wetland vertical change. *Limnology and Oceanography*. Vol. 63, Issue S1. https://doi.org/10.1002/lno.10783

Bruel, R. and Sabatier, P.: serac: an R package for ShortlivEd RAdionuclide chronology of recent sediment cores, *Journal of Environmental Radioactivity.* (2020) 225, 106449, https://doi.org/10.1016/j.jenvrad.2020.106449

Brush, G. S. (1984). Patterns of recent sediment accumulation in Chesapeake Bay (Virginia—Maryland, U.S.A.) tributaries. *Chemical Geology*. Vol. 44, Issues 1–3, pp. 227–242. https://doi.org/10.1016/0009-2541(84)90074-3

Cahoon, D. R., Reed, D. J., & Day, J. W., Jr. (1995). Estimating shallow subsidence in microtidal salt marshes of the southeastern United States: Kaye and Barghoorn revisited. *Marine Geology.* Vol. 128, Issues 1–2, pp. 1–9. https://doi.org/10.1016/0025-3227(95)00087-f

Cahoon, D. R. (2015). Estimating Relative Sea-Level Rise and Submergence Potential at a Coastal Wetland. *Estuaries and Coasts*. Vol. 38, Issue 3, pp. 1077–1084. https://doi.org/10.1007/s12237-014-9872-8

Cahoon, D. R., J. C. Lynch, P. Hensel, R. Boumans, B. C. Perez, B Segura and J. W. Day Jr. (2002a). High precision measurements of wetland sediment elevation: I. Recent improvements to the Sedimentation-Erosion Table. *Journal of Sedimentary Research* 72(5):730-733. https://doi.org/10.1306/020702720730

Cahoon, D. R., J. C. Lynch, B. C. Perez, B. Segura, R. Holland, C. Stelly, G. Stephenson, and P. Hensel (2002b). A device for high precision measurement of wetland sediment elevation: II. The rod surface elevation table. *Journal of Sedimentary Research* 72(5):734-739. https://doi.org/10.1306/020702720734

Cahoon, D. R., Lynch, J. C., Roman, C. T., Schmit, J. P., & Skidds, D. E. (2018). Evaluating the Relationship Among Wetland Vertical Development, Elevation Capital, Sea-Level Rise, and Tidal Marsh Sustainability. *Estuaries and Coasts*. Vol. 42, Issue 1, pp. 1–15. https://doi.org/10.1007/s12237-018-0448-x

Callaway, J. C., Cahoon, D. R., & Lynch, J. C. (2015). The Surface Elevation Table-Marker Horizon Method for Measuring Wetland Accretion and Elevation Dynamics. *Methods in Biogeochemistry of Wetlands* (pp. 901–917). https://doi.org/10.2136/sssabookser10.c46

Callaway, J.C., (1996) Sediment Accretion in Coastal Wetlands: A Review and A Simulation Model Process. *Current Topics in Wetland Biogeochemistry*. Vol 2, 1996 p. 2-23.

Cazenave, A., & Llovel, W. (2010). Contemporary Sea Level Rise. *Annual Review of Marine Science*. Vol. 2, Issue 1, pp. 145–173. https://doi.org/10.1146/annurev-marine-120308-081105

Chillrud, S. N., Bopp, R. F., Simpson, H. J., Ross, J. M., Shuster, E. L., Chaky, D. A., Walsh, D. C., Choy, C. C., Tolley, L.-R., & Yarme, A. (1999). Twentieth Century Atmospheric Metal Fluxes into Central Park Lake, New York City. *Environmental Science & Technology.* Vol. 33, Issue 5, pp. 657–662.https://doi.org/10.1021/es9807892

Chillrud, S. N., Hemming, S., Shuster, E. L., Simpson, H. J., Bopp, R. F., Ross, J. M., Pederson, D. C., Chaky, D. A., Tolley, L.-R., & Estabrooks, F. (2003). Stable lead isotopes, contaminant metals and radionuclides in upper Hudson River sediment cores: implications for improved time stratigraphy and transport processes. *Chemical Geology.* Vol. 199, Issues 1–2, pp. 53–70. https://doi.org/10.1016/s0009-2541(03)00055-x

Chillrud, S.N., Kenna, T.C., (2009) Identifying sources of non-fallout nuclear contamination in Hudson River sediments by plutonium and neptunium isotope ratios: sensitive tracers of sediment transport. Final report for project 003/03A, Hudson River Foundation No. HHF.CHI.1.10, New York.

Copple, S. P., Peteet, D. M., Balk, D., Chang, C., Jones, B., & Tzortziou, M. (2023). Marsh archive reveals human population history and future implications for estuarine health in Long Island Sound. *Science of The Total Environment.* Vol. 895, p. 164885. https://doi.org/10.1016/j.scitotenv.2023.164885

Courtney, S., Montalto, F., & Watson, E. B. (2023). Climate and Vegetation Change in a Coastal Marsh: Two Snapshots of Groundwater Dynamics and Tidal Flooding at Piermont Marsh, NY Spanning 20 Years. *Wetlands.* Vol. 44, Issue 1. https://doi.org/10.1007/s13157-023-01761-9

Cox Analytics. ITRAX Core Scanner (Accessed August 1 2023). https://www.coxsys.se/itrax core-scanner

Croudace and Rothwell (2015) *Micro-XRF Studies of Sediment Cores. Applications of a non-destructive tool for the environmental sciences.* Springer Publishing.

Davis, P. E. D., Nicholls, K. W., Holland, D. M., Schmidt, B. E., Washam, P., Riverman, K. L., Arthern, R. J., Vaňková, I., Eayrs, C., Smith, J. A., Anker, P. G. D., Mullen, A. D., Dichek, D., Lawrence, J. D., Meister, M. M., Clyne, E., Basinski-Ferris, A., Rignot, E., Queste, B. Y., … Makinson, K. (2023). Suppressed basal melting in the eastern Thwaites Glacier grounding zone. *Nature.* Vol. 614, Issue 7948, pp. 479–485. https://doi.org/10.1038/s41586-022-05586-0

Dean, W.E. (1974). Determination of Carbonate and Organic Matter in Calcareous Sediments and Sedimentary

Rocks by Loss on Ignition: Comparison With Other Methods. *Journal of Sedimentary Research*. Vol. 44. https://doi.org/10.1306/74d729d2-2b21-11d7-8648000102c1865d

Delaune, R. D., Patrick, W. H., JR, & Buresh, R. J. (1978). Sedimentation rates determined by 137Cs dating in a rapidly accreting salt marsh. *Nature.* Vol. 275, Issue 5680, pp. 532–533. https://doi.org/10.1038/275532a0

Doody, J. P. (2004). "Coastal Squeeze": An Historical Perspective. *Journal of Coastal Conservation*, *10*(1/2), 129–138. http://www.jstor.org/stable/25098445

Dubossi, D., Gibson, A., Jeanpierre, D., Dorsey, T., Mapp, N., Parra, E., Ojeda, K., Adorno, Y. (2015) Sediment deposition and accretion in a Hudson River tidal marsh. 2015 GSA Annual Meeting in Baltimore, Maryland, US. 1-3 November 2015. Geological Society of America. Abstracts with Programs. Vol 47, No 7, p.327.

Dunnington, D. W., Roberts, S., Norton, S. A., Spooner, I. S., Kurek, J., Kirk, J. L., Muir, D. C. G., White, C. E., & Gagnon, G. A. (2020). The distribution and transport of lead over two centuries as recorded by lake sediments from northeastern North America. *Science of The Total Environment.* Vol. 737, p. 140212. https://doi.org/10.1016/j.scitotenv.2020.140212

Drexler, J. Z., Woo, I., Fuller, C. C., & Nakai, G. (2019). Carbon accumulation and vertical accretion in a restored versus historic salt marsh in southern Puget Sound, Washington, United States. *Restoration Ecology*. Vol. 27, Issue 5, pp. 1117–1127. https://doi.org/10.1111/rec.12941

Edgington, D. N., & Robbins, J. A. (1976). Records of lead deposition in Lake Michigan sediments since 1800. *Environmental Science & Technology.* Vol. 10, Issue 3, pp. 266–274. https://doi.org/10.1021/es60114a007

Engelhart, S. E., & Horton, B. P. (2012). Holocene sea level database for the Atlantic coast of the United States. In Quaternary Science Reviews (Vol. 54, pp. 12–25). Elsevier BV. https://doi.org/10.1016/j.quascirev.2011.09.013

Faegri, K. & Iversen, J. (1975) *Textbook of Pollen Analysis.* Third edition, Hafner, New York.

Fagherazzi, S., Mariotti, G., Leonardi, N., Canestrelli, A., Nardin, W., & Kearney, W. S. (2020). Salt Marsh Dynamics in a Period of Accelerated Sea Level Rise. *Journal of Geophysical Research: Earth Surface*. Vol. 125, Issue 8. https://doi.org/10.1029/2019jf005200

Farmer, J. G. (1978). Lead concentration profiles in lead-210 dated Lake Ontario sediment cores. *Science of The Total Environment.* Vol. 10, Issue 2, pp. 117–127. https://doi.org/10.1016/0048-9697(78)90057-8

Foucher, A., Chaboche, P.-A., Sabatier, P., and Evrard, O. (2021). A worldwide meta-analysis (1977 2020) of sediment core dating using fallout radionuclides including ^{137}Cs and $^{210}Pb_{xs}$, *Earth System Science Data.* 13, 4951–4966. https://doi.org/10.5194/essd-13-4951-2021

Fluet-Chouinard, E., Stocker, B. D., Zhang, Z., Malhotra, A., Melton, J. R., Poulter, B., Kaplan, J. O., Goldewijk, K. K., Siebert, S., Minayeva, T., Hugelius, G., Joosten, H., Barthelmes, A., Prigent, C., Aires, F., Hoyt, A. M., Davidson, N., Finlayson, C. M., Lehner, B., … McIntyre, P. B. (2023). Extensive global wetland loss over the past three centuries. *Nature.* Vol. 614, Issue 7947, pp. 281–286. https://doi.org/10.1038/s41586-022-05572-6

Goodman, J. E., Wood, M. E., & Gehrels, W. R. (2007). A 17-yr record of sediment accretion in the salt marshes of Maine (USA). *Marine Geology*. Vol. 242, Issues 1–3, pp. 109–121. https://doi.org/10.1016/j.margeo.2006.09.017

Gomez, N., Mitrovica, J. X., Tamisiea, M. E., & Clark, P. U. (2010). A new projection of sea level change in response to collapse of marine sectors of the Antarctic Ice Sheet. *Geophysical Journal International* (Vol. 180, Issue 2, pp. 623–634). https://doi.org/10.1111/j.1365-246x.2009.04419.x

Gornitz, V., Oppenheimer, M., Kopp, R., Orton, P., Buchanan, M., Lin, N., Horton, R., & Bader, D. (2020). *Sea level rise*. In C. Rosenzweig & W. Solecki (Eds.), *New York City Panel on Climate Change 2019 Report* (Chapter 3). Annals of the New York Academy of Sciences. https://doi.org/10.1016/j.uclim.2020.100654

Graney, J. R., Halliday, A. N., Keeler, G. J., Nriagu, J. O., Robbins, J. A., & Norton, S. A. (1995). Isotopic record of lead pollution in lake sediments from the northeastern United States. *Geochimica et Cosmochimica Acta.* Vol. 59, Issue 9, pp. 1715–1728. https://doi.org/10.1016/0016-7037(95)00077-d

Grünfeld, S., & Brix, H. (1999). Methanogenesis and methane emissions: effects of water table, substrate type and presence of Phragmites australis. *Aquatic Botany.* Vol. 64, Issue 1, pp. 63–75. https://doi.org/10.1016/s0304-3770(99)00010-8

Haaf, L., Watson, E. B., Elsey-Quirk, T., Raper, K., Padeletti, A., Maxwell-Doyle, M., Kreeger, D., & Velinsky, D. J. (2021). Sediment Accumulation, Elevation Change, and the Vulnerability of Tidal Marshes in the Delaware Estuary and Barnegat Bay to Accelerated Sea Level Rise. *Estuaries and Coasts.* Vol. 45, Issue 2, pp. 413–427. https://doi.org/10.1007/s12237-021-00972-9

Hein, C. J., Connell, J. E., FitzGerald, D. M., Georgiou, I. Y., Hughes, Z. J., & King, K. (2024). Vertical accretion

trends project doughnut-like fragmentation of saltmarshes. *Communications Earth & Environment* (Vol. 5, Issue 1). https://doi.org/10.1038/s43247-024-01219-8

Herron, E. M., Dorman, J., & Drake, C. L. (1968). Seismic study of the sediments in the Hudson River. *Journal of Geophysical Research*. Vol. 73, Issue 14, pp. 4701–4709. https://doi.org/10.1029/jb073i014p04701

Hill, T. D., & Anisfeld, S. C. (2015). Coastal wetland response to sea level rise in Connecticut and New York. *Estuarine, Coastal and Shelf Science.* Vol. 163, pp. 185–193. https://doi.org/10.1016/j.ecss.2015.06.004

Holmquist, J. R., Brown, L. N., & MacDonald, G. M. (2021). Localized Scenarios and Latitudinal Patterns of Vertical and Lateral Resilience of Tidal Marshes to Sea-Level Rise in the Contiguous United States. *Earth's Future.* Vol. 9, Issue 6. https://doi.org/10.1029/2020ef001804

Horton, R., Little, C., Gornitz, V., Bader, D., & Oppenheimer, M. (2015). New York City Panel on Climate Change 2015 Report Chapter 2: Sea Level Rise and Coastal Storms. *Annals of the New York Academy of Sciences.* Vol. 1336, Issue 1, pp. 36–44. https://doi.org/10.1111/nyas.12593

Howarth, R. W., & Hobbie, J. E. (1982). The Regulation of Decomposition and Heterotrophic Microbial Activity in Salt Marsh Soils: A Review. *Estuarine Comparisons*. pp. 183–207. https://doi.org/10.1016/b978-0-12-404070-0.50017-x

Kearney, M. S., & Ward, L. G. (1986). Accretion rates in brackish marshes of a Chesapeake Bay estuarine tributary. *Geo-Marine Letters*. Vol. 6, Issue 1, pp. 41–49. https://doi.org/10.1007/bf02311695

Jowsey, P.C. (1966) An improved peat sampler. *New Phytologist,* 65, 245–248.

Kaye, C. A., & Barghoon, E. S. (1964). Late Quaternary Sea-Level Change and Crustal Rise at Boston, Massachusetts, with Notes on the Autocompaction of Peat. *Geological Society of America Bulletin.* Vol. 75, Issue 2, p. 63. https://doi.org/10.1130/0016-7606(1964)75[63:lqscac]2.0.co;2

Kearney, M. S., & Ward, L. G. (1986). Accretion rates in brackish marshes of a Chesapeake Bay estuarine tributary. *Geo-Marine Letters*. Vol. 6, Issue 1, pp. 41–49). https://doi.org/10.1007/bf02311695

Kemp, A. C., Horton, B. P., Donnelly, J. P., Mann, M. E., Vermeer, M., & Rahmstorf, S. (2011). Climate related sea-level variations over the past two millennia. *Proceedings of the National Academy of Sciences.* Vol. 108, Issue 27, pp. 11017–11022. https://doi.org/10.1073/pnas.1015619108

Kemp, A. C., Hill, T. D., Vane, C. H., Cahill, N., Orton, P. M., Talke, S. A., Parnell, A. C., Sanborn, K., & Hartig, E. K. (2017). Relative sea-level trends in New York City during the past 1500 years. *The Holocene.* Vol. 27, Issue 8, pp. 1169–1186. https://doi.org/10.1177/0959683616683263

Kenna, T. C., Nitsche, F. O., Herron, M. M., Mailloux, B. J., Peteet, D., Sritrairat, S., Sands, E., & Baumgarten, J. (2011). Evaluation and calibration of a Field Portable X-Ray Fluorescence spectrometer for quantitative analysis of siliciclastic soils and sediments. *Journal of Analytic Atomic Spectroscopy*. Vol. 26, Issue 2, pp. 395–405. https://doi.org/10.1039/c0ja00133c

Kirwan, M. L., & Megonigal, J. P. (2013). Tidal wetland stability in the face of human impacts and sea-level rise. *Nature.* Vol. 504, Issue 7478, pp. 53–60. https://doi.org/10.1038/nature12856

Kirwan, M. L., Guntenspergen, G. R., & Langley, J. A. (2014). Temperature sensitivity of organic-matter decay in tidal marshes. *Biogeosciences.* Vol. 11, Issue 17, pp. 4801–4808. https://doi.org/10.5194/bg-11-4801-2014

Kirwan, M. L., Temmerman, S., Skeehan, E. E., Guntenspergen, G. R., & Fagherazzi, S. (2016). Overestimation of marsh vulnerability to sea level rise. *Nature Climate Change*. Vol. 6, Issue 3, pp. 253–260. https://doi.org/10.1038/nclimate2909

Kirwan, M. L., Temmerman, S., Guntenspergen, G. R., & Fagherazzi, S. (2017). Reply to "Marsh vulnerability to sea-level rise." *Nature Climate Change*. Vol. 7, Issue 11, pp. 756–757. https://doi.org/10.1038/nclimate3425

Kopp, R. E., Horton, R. M., Little, C. M., Mitrovica, J. X., Oppenheimer, M., Rasmussen, D. J., Strauss, B. H., & Tebaldi, C. (2014). Probabilistic 21st and 22nd century sea-level projections at a global network of tide-gauge sites. *Earth's Future.* Vol. 2, Issue 8, pp. 383–406. https://doi.org/10.1002/2014ef000239

Lacy, J. R., Foster-Martinez, M. R., Allen, R. M., Ferner, M. C., & Callaway, J. C. (2020). Seasonal Variation in Sediment Delivery Across the Bay-Marsh Interface of an Estuarine Salt Marsh. Journal of Geophysical Research: Oceans (Vol. 125, Issue 1). https://doi.org/10.1029/2019jc015268

Lima, A. L., Bergquist, B. A., Boyle, E. A., Reuer, M. K., Dudas, F. O., Reddy, C. M., & Eglinton, T. I. (2005). High-resolution historical records from Pettaquamscutt River basin sediments: 2. Pb isotopes reveal a potential new stratigraphic marker. *Geochimica et Cosmochimica Acta.* Vol. 69, Issue 7, pp. 1813–1824. https://doi.org/10.1016/j.gca.2004.10.008

Lynch, J. C., P. Hensel, and D. R. Cahoon (2015). The surface elevation table and marker horizon technique: A protocol for monitoring wetland elevation dynamics. Natural Resource Report NPS/NCBN/NRR—2015/1078. National Park Service, Fort Collins, Colorado.

MacKenzie, R. A., Krauss, K. W., Cormier, N., Eperiam, E., van Aardt, J., Kargar, A. R., Grow, J., & Klump, J. V. (2023). Relative Effectiveness of a Radionuclide (210Pb), Surface Elevation Table (SET), and LiDAR At Monitoring Mangrove Forest Surface Elevation Change. *Estuaries and Coasts.* https://doi.org/10.1007/s12237-023-01301-y

Maher, N., & Starke, A. (2023). Suboptimal Rootzone Growth Prevents Long Island (NY) Salt Marshes from Keeping Pace with Sea Level Rise. *Estuaries and Coasts.* https://doi.org/10.1007/s12237-023-01295-7

Maxwell, T. L., Rovai, A. S., Adame, M. F., Adams, J. B., Álvarez-Rogel, J., Austin, W. E. N., Beasy, K., Boscutti, F., Böttcher, M. E., Bouma, T. J., Bulmer, R. H., Burden, A., Burke, S. A., Camacho, S., Chaudhary, D. R., Chmura, G. L., Copertino, M., Cott, G. M., Craft, C., … Worthington, T. A. (2023). Global dataset of soil organic carbon in tidal marshes. *Scientific Data.* Vol. 10, Issue 1. https://doi.org/10.1038/s41597-023-02633-x

Miller, K. G., Kopp, R. E., Horton, B. P., Browning, J. V., & Kemp, A. C. (2013). A geological perspective on sea-level rise and its impacts along the U.S. mid-Atlantic coast. *Earth's Future.* Vol. 1, Issue 1, pp. 3–18. https://doi.org/10.1002/2013ef000135

Mitrovica, J. X., Gomez, N., & Clark, P. U. (2009). The Sea-Level Fingerprint of West Antarctic Collapse. *Science.* Vol. 323, Issue 5915, pp. 753–753. https://doi.org/10.1126/science.1166510

Molino, G. D., Carr, J. A., Ganju, N. K., & Kirwan, M. L. (2022). Variability in marsh migration potential determined by topographic rather than anthropogenic constraints in the Chesapeake Bay region. *Limnology and Oceanography Letters*. Vol. 7, Issue 4, pp. 321–331. https://doi.org/10.1002/lol2.10262

Montalto, F. A., Steenhuis, T. S., & Parlange, J.-Y. (2006). The hydrology of Piermont Marsh, a reference for tidal marsh restoration in the Hudson river estuary, New York. *Journal of Hydrology.* Vol. 316, Issues 1–4, pp. 108–128. https://doi.org/10.1016/j.jhydrol.2005.03.043

Morris, J. T., Sundareshwar, P. V., Nietch, C. T., Kjerfve, B., & Cahoon, D. R. (2002). Responses of Coastal Wetlands to Rising Sea Level. *Ecology* (Vol. 83, Issue 10, pp. 2869–2877). https://doi.org/10.1890/0012-9658(2002)083[2869:rocwtr]2.0.co;2

Morris, J. T., Barber, D. C., Callaway, J. C., Chambers, R., Hagen, S. C., Hopkinson, C. S., Johnson, B. J., Megonigal, P., Neubauer, S. C., Troxler, T., & Wigand, C. (2016). Contributions of organic and inorganic matter to sediment volume and accretion in tidal wetlands at steady state. *Earth's Future.* Vol. 4, Issue 4, pp. 110–121. https://doi.org/10.1002/2015ef000334

Najjar, R. G., Herrmann, M., Alexander, R., Boyer, E. W., Burdige, D. J., Butman, D., Cai, W. -J., Canuel, E. A., Chen, R. F., Friedrichs, M. A. M., Feagin, R. A., Griffith, P. C., Hinson, A. L., Holmquist, J. R., Hu, X., Kemp, W. M., Kroeger, K. D., Mannino, A., McCallister, S. L., ··· Zimmerman, R. C. (2018). Carbon Budget of Tidal Wetlands, Estuaries, and Shelf Waters of Eastern North America. Global Biogeochemical Cycles, 32(3), 389–416. https://doi.org/10.1002/2017gb005790

New York State Department of Environmental Conservation (NYSDEC). Hudson River National Estuarine Research Reserve Management Plan (Albany, 2019).

Nitsche, F. O., Kenna, T. C., & Haberman, M. (2010). Quantifying 20th century deposition in complex estuarine environment: An example from the Hudson River. *Estuarine, Coastal and Shelf Science*. Vol. 89, Issue 2, pp. 163–174. https://doi.org/10.1016/j.ecss.2010.06.011

Nitsche F.O., and Kenna, T.C. (2018) Assessing Impact of Recent Storm Activity and Sediment Transport and Storage in the Hudson River. Hudson River Foundation Final Report Grant 006/13A. https://www.hudsonriver.org/wp-content/uploads/library/Nitsche_and_Kenna_008_05A_final_report.pdf

Olsen, C.R., Simpson, H.J., Bopp, R.F., Williams, S.C., Peng, T.H. & Deck, B. L. (1978) A geochemical analysis of the sediments and sedimentation in the Hudson Estuary. *Journal of Sedimentary Research*, 48, 401–418. https://doi.org/10.1306/212F7496-2B24-11D7-8648000102C1865D

Page, R.A., Molnar, P.H., Oliver, J. (1968) Seismicity in the Vicinity of the Ramapo Fault, New Jersey-New York. *Bulletin of the Seismological Society of America.* Vol 58, No 2, pp. 681-687.

Parkinson, R. W., Craft, C., DeLaune, R. D., Donoghue, J. F., Kearney, M., Meeder, J. F., Morris, J., & Turner, R. E. (2017). Marsh vulnerability to sea-level rise. *Nature Climate Change.* Vol. 7, Issue 11, pp. 756–756. https://doi.org/10.1038/nclimate3424

Pederson, D. C., Peteet, D. M., Kurdyla, D., & Guilderson, T. (2005). Medieval Warming, Little Ice Age, and European impact on the environment during the last millennium in the lower Hudson Valley, New York, USA. *Quaternary Research.* Vol. 63, Issue 3, pp. 238–249. https://doi.org/10.1016/j.yqres.2005.01.001

Peltier, W. R. (1996). Global sea level rise and glacial isostatic adjustment: An analysis of data from the East Coast

of North America. *Geophysical Research Letters.* Vol. 23, Issue 7, pp. 717–720. https://doi.org/10.1029/96gl00848

Peltier, W. R. (2004). Global Glacial Isostasy and the Surface of the Ice-Age Earth: The ICE-5G (VM2) Model and GRACE. *Annual Review of Earth and Planetary Sciences*. Vol. 32, Issue 1, pp. 111–149. https://doi.org/10.1146/annurev.earth.32.082503.144359

Peltier, W. R., & Fairbanks, R. G. (2006). Global glacial ice volume and Last Glacial Maximum duration from an extended Barbados sea level record. *Quaternary Science Reviews*. Vol. 25, Issues 23–24, pp. 3322–3337. https://doi.org/10.1016/j.quascirev.2006.04.010

Peteet, D., Nichols, J., Pederson, D., Kenna, T., Chang, C., Newton, B., & Vincent, S. (2020). Climate and anthropogenic controls on blue carbon sequestration in Hudson River tidal marsh, Piermont, New York. *Environmental Research Letters*. Vol. 15, Issue 6, p. 065001. https://doi.org/10.1088/1748-9326/ab7a56

Peteet, D. M., Nichols, J., Kenna, T., Chang, C., Browne, J., Reza, M., Kovari, S., Liberman, L., & Stern-Protz, S. (2018). Sediment starvation destroys New York City marshes' resistance to sea level rise. *Proceedings of the National Academy of Sciences*. Vol. 115, Issue 41, pp. 10281–10286.https://doi.org/10.1073/pnas.1715392115

Peteet, D.M., D.C. Pederson, D. Kurdyla, and T. Guilderson (2007) Hudson River paleoecology from marshes: Environmental change and its implications for fisheries. In *Hudson River Fishes and Their Environment*, A.F.S. Symposium 51. J.R. Waldman, K.E. Limburg, and D. Strayer, Eds., American Fisheries Society, pp. 112-128.

Ralston, D. K., Yellen, B., Woodruff, J. D., & Fernald, S. (2020a). Turbidity Hysteresis in an Estuary and Tidal River Following an Extreme Discharge Event. *Geophysical Research Letters.* Vol. 47, Issue 15. https://doi.org/10.1029/2020gl088005

Ralston, D. K., Yellen, B., & Woodruff, J. D. (2020b). Watershed sediment supply and potential impacts of dam removals for an estuary. https:// doi.org/10.1002/essoar.10502519.1.ESSOAr

Ralston, D. K., Yellen, B., & Woodruff, J. D. (2021). Watershed Suspended Sediment Supply and Potential Impacts of Dam Removals for an Estuary. *Estuaries and Coasts.* Vol. 44, Issue 5, pp. 1195–1215. https://doi.org/10.1007/s12237-020-00873-3

Raposa, K. B., Woolfolk, A., Endris, C. A., Fountain, M. C., Moore, G., Tyrrell, M., Swerida, R., Lerberg, S., Puckett, B. J., Ferner, M. C., Hollister, J., Burdick, D. M., Champlin, L., Krause, J. R., Haines, D., Gray, A. B., Watson, E. B., & Wasson, K. (2023). Evaluating Thin-Layer Sediment Placement as a Tool for Enhancing Tidal Marsh Resilience: a Coordinated Experiment Across Eight US National Estuarine Research Reserves. *Estuaries and Coasts.* Vol. 46, Issue 3, pp. 595–615. https://doi.org/10.1007/s12237-022-01161-y

Raposa, K. B., Cole Ekberg, M. L., Burdick, D. M., Ernst, N. T., & Adamowicz, S. C. (2016). Elevation change and the vulnerability of Rhode Island (USA) salt marshes to sea-level rise. *Regional Environmental Change*. Vol. 17, Issue 2, pp. 389–397. https://doi.org/10.1007/s10113-016-1020-5

Redfield, A. C. (1967). Postglacial Change in Sea Level in the Western North Atlantic Ocean. *Science.* Vol. 157, Issue 3789, pp. 687–692. https://doi.org/10.1126/science.157.3789.687

Redfield, A. C. (1972). Development of a New England Salt Marsh. *Ecological Monographs.* Vol. 42, Issue 2, pp. 201–237. https://doi.org/10.2307/1942263

Riverkeeper (2022) Sparkill PEERS Water Quality Monitoring Final Report. https://www.riverkeeper.org/wp-content/uploads/2022/06/Sparkill-PEERS-Water-Quality-Monitoring-Final-Report.pdf

Rogers, K., Kelleway, J. J., Saintilan, N., Megonigal, J. P., Adams, J. B., Holmquist, J. R., Lu, M., Schile-Beers, L., Zawadzki, A., Mazumder, D., & Woodroffe, C. D. (2019). Wetland carbon storage controlled by millennial-scale variation in relative sea-level rise. *Nature.* Vol. 567, Issue 7746, pp. 91–95. https://doi.org/10.1038/s41586-019-0951-7

Rooth, J. E., & Stevenson, J. C. (2000). *Wetlands Ecology and Management.* Vol. 8, Issue 2/3, pp. 173–183. https://doi.org/10.1023/a:1008444502859

Roman, C. T., Lynch, J. C., & Cahoon, D. R. (2023). Twenty-Year Record of Salt Marsh Elevation Dynamics in Response to Sea-Level Rise and Storm-Driven Barrier Island Geomorphic Processes: Fire Island, NY, USA. *Estuaries and Coasts.* https://doi.org/10.1007/s12237-023-01234-6

Roman, C.T., J.W. King, D.R. Cahoon, J.C. Lynch, and P.G. Appleby. 2007. Evaluation of marsh development processes at Fire Island National Seashore (New York): recent and historic perspectives. National Park Service, Northeast Region, Boston, MA. Technical Report NPS/NER/NRTR – 2007/089. 62p. https://irma.nps.gov/DataStore/Reference/Profile/2181170

Rovere, A., Stocchi, P., & Vacchi, M. (2016). Eustatic and Relative Sea Level Changes. *Current Climate Change Reports*. Vol. 2, Issue 4, pp. 221–231. https://doi.org/10.1007/s40641-016-0045-7

Sadler, P. M. (1981). Sediment Accumulation Rates and the Completeness of Stratigraphic Sections. *The Journal of Geology* (Vol. 89, Issue 5, pp. 569–584). https://doi.org/10.1086/628623

Saintilan, N., Kovalenko, K. E., Guntenspergen, G., Rogers, K., Lynch, J. C., Cahoon, D. R., Lovelock, C. E., Friess, D. A., Ashe, E., Krauss, K. W., Cormier, N., Spencer, T., Adams, J., Raw, J., Ibanez, C., Scarton, F., Temmerman, S., Meire, P., Maris, T., … Khan, N. (2022). Constraints on the adjustment of tidal marshes to accelerating sea level rise. In Science (Vol. 377, Issue 6605, pp. 523–527). American Association for the Advancement of Science (AAAS). https://doi.org/10.1126/science.abo7872

Saintilan, N., Horton, B., Törnqvist, T. E., Ashe, E. L., Khan, N. S., Schuerch, M., Perry, C., Kopp, R. E., Garner, G. G., Murray, N., Rogers, K., Albert, S., Kelleway, J., Shaw, T. A., Woodroffe, C. D., Lovelock, C. E., Goddard, M. M., Hutley, L. B., Kovalenko, K., … Guntenspergen, G. (2023). Widespread retreat of coastal habitat is likely at warming levels above 1.5 °C. *Nature.* Vol. 621, Issue 7977, pp. 112–119. https://doi.org/10.1038/s41586-023-06448-z

Sallenger, A. H., Jr, Doran, K. S., & Howd, P. A. (2012). Hotspot of accelerated sea-level rise on the Atlantic coast of North America. *Nature Climate Change*. Vol. 2, Issue 12, pp. 884–888. https://doi.org/10.1038/nclimate1597

Schoot, P. M. and J. E. A. de Jong. 1982. Sedimentatie en erosiemetingen met behulp van de Sedi-Eros-Tafel (Set). Ministerie van verfkeer en waterstaat, rijkswaterstaat. Note # DDMI-82.401.

Sheng, Y. P., Rivera-Nieves, A. A., Zou, R., Paramygin, V. A., Angelini, C., & Sharp, S. J. (2021). Invasive Phragmites provides superior wave and surge damage protection relative to native plants during storms. *Environmental Research Letters*. Vol. 16, Issue 5, p. 054008. https://doi.org/10.1088/1748-9326/abf288

Sheng, Y. P., Rivera-Nieves, A. A., Zou, R., & Paramygin, V. A. (2021). Role of wetlands in reducing structural loss is highly dependent on characteristics of storms and local wetland and structure conditions. *Scientific Reports*. Vol. 11, Issue 1. https://doi.org/10.1038/s41598-021-84701-z

Sheng, Y. P., Paramygin, V. A., Rivera-Nieves, A. A., Zou, R., Fernald, S., Hall, T., & Jacob, K. (2022). Coastal marshes provide valuable protection for coastal communities from storm-induced wave, flood, and structural loss in a changing climate. *Scientific Reports*. Vol. 12, Issue 1. https://doi.org/10.1038/s41598-022-06850-z

Simpson, H. J.; Olsen, C. R.; Williams, S. C.; Trier, R. M. (1976) *Science,* 179-83. https://doi.org/10.1126/science.959844

Sommerfield, C. K. (2006). On sediment accumulation rates and stratigraphic completeness: Lessons from Holocene ocean margins. *Continental Shelf Research*. Vol. 26, Issues 17–18, pp. 2225–2240. https://doi.org/10.1016/j.csr.2006.07.015

Smeaton, C., Barlow, N. L. M., & Austin, W. E. N. (2020). Coring and compaction: Best practice in blue carbon stock and burial estimations. *Geoderma.* Vol. 364, p. 114180. https://doi.org/10.1016/j.geoderma.2020.114180

Steinmuller, H. E., Dittmer, K. M., White, J. R., & Chambers, L. G. (2019). Understanding the fate of soil organic matter in submerging coastal wetland soils: A microcosm approach. *Geoderma.* Vol. 337, pp. 1267–1277. https://doi.org/10.1016/j.geoderma.2018.08.020

Steinmuller, H. E., & Chambers, L. G. (2019). Characterization of coastal wetland soil organic matter: Implications for wetland submergence. *Science of The Total Environment*. Vol. 677, pp. 648–659. https://doi.org/10.1016/j.scitotenv.2019.04.405

Sritrairat (2013) *Multiproxy Analyses of Past Vegetation, Climate, and sediment dynamics in Hudson River Wetlands*. Columbia University PhD Thesis.

Sritrairat, S., Peteet, D. M., Kenna, T. C., Sambrotto, R., Kurdyla, D., & Guilderson, T. (2012). A history of vegetation, sediment and nutrient dynamics at Tivoli North Bay, Hudson Estuary, New York. *Estuarine, Coastal and Shelf Science*. Vols. 102–103, pp. 24–35. Elsevier BV. https://doi.org/10.1016/j.ecss.2012.03.003

Tabak, N. M., Laba, M., & Spector, S. (2016). Simulating the Effects of Sea Level Rise on the Resilience and Migration of Tidal Wetlands along the Hudson River. *PLOS ONE.* Vol. 11, Issue 4, p. e0152437. https://doi.org/10.1371/journal.pone.0152437

Tonitto, C., & Riha, S. J. (2016). Planning and implementing small dam removals: lessons learned from dam removals across the eastern United States. Sustainable Water Resources Management. Vol. 2, Issue 4, pp. 489–507. https://doi.org/10.1007/s40899-016-0062-7

Tweel, A. W., & Turner, R. E. (2014). Contribution of tropical cyclones to the sediment budget for coastal wetlands

in Louisiana, USA. *Landscape Ecology.* Vol. 29, Issue 6, pp. 1083–1094. https://doi.org/10.1007/s10980-014-0047-6

USGS (2024) https://earthquake.usgs.gov/earthquakes/eventpage/at00sbh3yv/executive

Valiela, I., Lloret, J., Bowyer, T., Miner, S., Remsen, D., Elmstrom, E., Cogswell, C., & Robert Thieler, E. (2018). Transient coastal landscapes: Rising sea level threatens salt marshes. *Science of The Total Environment.* Vols. 640–641, pp. 1148–1156. https://doi.org/10.1016/j.scitotenv.2018.05.235

Varekamp, J., Kreulen, B., ten Brink, B. M., & Mecray, E. (2003). Mercury contamination chronologies from Connecticut wetlands and Long Island Sound sediments. *Environmental Geology*. Vol. 43, Issue 3, pp. 268–282. https://doi.org/10.1007/s00254-002-0624-x

Vane, C. H., Kim, A. W., Moss-Hayes, V., Turner, G., Mills, K., Chenery, S. R., Barlow, T. S., Kemp, A. C., Engelhart, S. E., Hill, T. D., Horton, B. P., & Brain, M. (2020). Organic pollutants, heavy metals and toxicity in oil spill impacted salt marsh sediment cores, Staten Island, New York City, USA. *Marine Pollution Bulletin*. Vol. 151, p. 110721. https://doi.org/10.1016/j.marpolbul.2019.110721

Vaughn, D. R., Bianchi, T. S., Shields, M. R., Kenney, W. F., & Osborne, T. Z. (2020). Increased Organic Carbon Burial in Northern Florida Mangrove-Salt Marsh Transition Zones. *Global Biogeochemical Cycles.* Vol. 34, Issue 5.

Wall, G., Nystrom, E., & Litten, S. (2008). Suspended sediment transport in the freshwater reach of the Hudson River estuary in eastern New York. *Estuaries and Coasts,* 31(3), 542–553. https://doi.org/10.1007/s12237-008-9050-y

Webb, E. L., Friess, D. A., Krauss, K. W., Cahoon, D. R., Guntenspergen, G. R., & Phelps, J. (2013). A global standard for monitoring coastal wetland vulnerability to accelerated sea-level rise. *Nature Climate Change*. Vol. 3, Issue 5, pp. 458–465. https://doi.org/10.1038/nclimate1756

Wells, A. W., Nieder, W. C., Swift, B. L., O'Connor, K. A., & Weiss, C. A. (2008). Temporal Changes in the Breeding Bird Community at Four Hudson River Tidal Marshes. *Journal of Coastal Research*. Vol. 10055, pp. 221–235. https://doi.org/10.2112/si55-018.1

Weis, P., Barrett, K. R., Proctor, T., & Bopp, R. F. (2005). Studies of a contaminated brackish marsh in the Hackensack Meadowlands of northeastern New Jersey: An assessment of natural recovery. *Marine Pollution Bulletin.* Vol. 50, Issue 11, pp. 1405–1415. https://doi.org/10.1016/j.marpolbul.2005.06.013

Weis, J. S., Watson, E. B., Ravit, B., Harman, C., & Yepsen, M. (2021). The status and future of tidal marshes in New Jersey faced with sea level rise. *Anthropocene Coasts* (Vol. 4, Issue 1, pp. 168–192). https://doi.org/10.1139/anc-2020-0020

Wenning, R. J., Bonnevie, N. L., & Huntley, S. L. (1994). Accumulation of metals, polychlorinated biphenyls, and polycyclic aromatic hydrocarbons in sediments from the lower Passaic River, New Jersey. *Archives of Environmental Contamination and Toxicology.* Vol. 27, Issue 1. https://doi.org/10.1007/bf00203890

Wiberg, P. L., Fagherazzi, S., & Kirwan, M. L. (2020). Improving Predictions of Salt Marsh Evolution Through Better Integration of Data and Models. *Annual Review of Marine Science.* Vol. 12, Issue 1, pp. 389–413. https://doi.org/10.1146/annurev-marine-010419-010610

Wigand, C., Roman, C. T., Davey, E., Stolt, M., Johnson, R., Hanson, A., Watson, E. B., Moran, S. B., Cahoon, D. R., Lynch, J. C., & Rafferty, P. (2014). Below the disappearing marshes of an urban estuary: historic nitrogen trends and soil structure. *Ecological Applications*. Vol. 24, Issue 4, pp. 633–649. https://doi.org/10.1890/13-0594.1

Worzel, J. L., & Drake, C. L. (1959). Structure Section Across the Hudson River at Nyack, NY from Seismic Observations. *Annals of the New York Academy of Sciences*. Vol. 80, Issue 4, pp. 1092–1105. https://doi.org/10.1111/j.1749-6632.1959.tb49282.x

Wright, A. J., Edwards, R. J., van de Plassche, O., Blaauw, M., Parnell, A. C., van der Borg, K., de Jong, A. F. M., Roe, H. M., Selby, K., & Black, S. (2017). Reconstructing the accumulation history of a saltmarsh sediment core: Which age-depth model is best? *Quaternary Geochronology.* Vol. 39, pp. 35–67. https://doi.org/10.1016/j.quageo.2017.02.004

Wu, W. and Knack, I. (2015) Assessment of Sediments Impounded by the Burden Pond Dam on the Wynats Kill Creek of New York. Technical Report. NYS Water Resources institute at Cornell University and the NYS Dec Hudson River Estuary Program.

Wu, W., Knack, I., and Perera, C. (2016) Prediction of Sediment Remobilized by Removal of the Bingham Mills Dam in the Hudson River Watershed. Technical Report. NYS Water Resources institute at Cornell University and the NYS Dec Hudson River Estuary Program.

Yao, Q., Liu, K., Platt, W. J., & Rivera-Monroy, V. H. (2015). Palynological reconstruction of environmental

changes in coastal wetlands of the Florida Everglades since the mid-Holocene. *Quaternary Research.* Vol. 83, Issue 3, pp. 449–458. https://doi.org/10.1016/j.yqres.2015.03.005

Yellen, B., Woodruff, J., Ladlow, C., Ralston, D. K., Fernald, S., & Lau, W. (2020). Rapid tidal marsh development in anthropogenic backwaters. *Earth Surface Processes and Landforms.* Vol. 46, Issue 3, pp. 554–572. https://doi.org/10.1002/esp.5045

Yin, J., Schlesinger, M. E., & Stouffer, R. J. (2009). Model projections of rapid sea-level rise on the northeast coast of the United States. *Nature Geoscience*. Vol. 2, Issue 4, pp. 262–266. https://doi.org/10.1038/ngeo462

Yohn, S., Long, D., Fett, J., & Patino, L. (2004). Regional versus local influences on lead and cadmium loading to the Great Lakes region. *Applied Geochemistry.* Vol. 19, Issue 7, pp. 1157–1175. https://doi.org/10.1016/j.apgeochem.2004.01.013

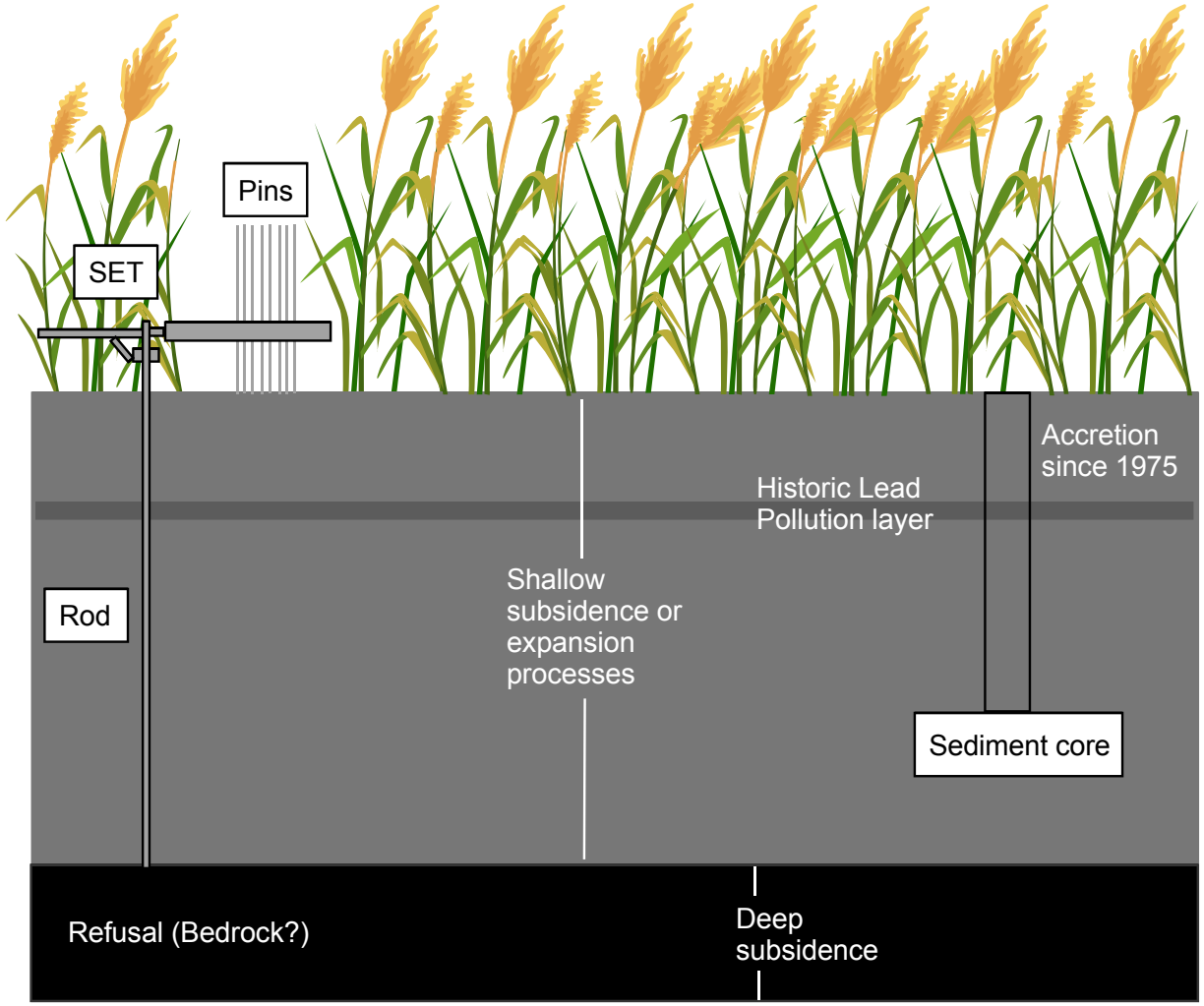

Figure 1. Figure 1. Schematic of RSET setup and subsurface processes that effect elevation change; use of historic markers to calculate accretion rates from sediment cores. Modified from Cahoon et al. (2015).

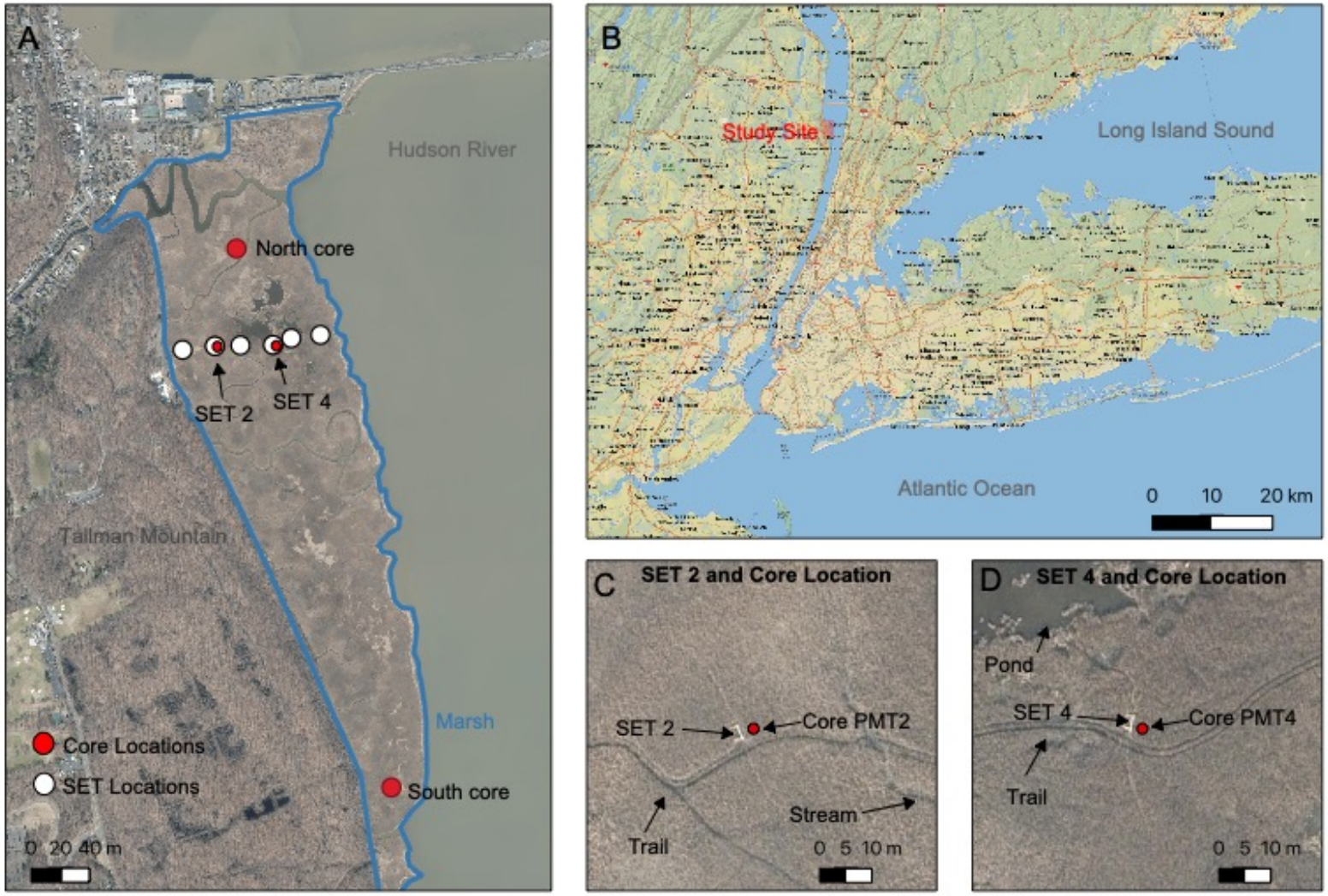

Figure 2. Map of study site. A, Map of Piermont Marsh, core locations, SET locations, and extent of the marsh. B, Regional map showing location of the study site, Atlantic Ocean and Long Island Sound. C, SET 2 and nearby core location (PMT2) map, with trail and stream labeled. D, SET 4 and nearby core location map (PMT 4), with trail and stream labeled.

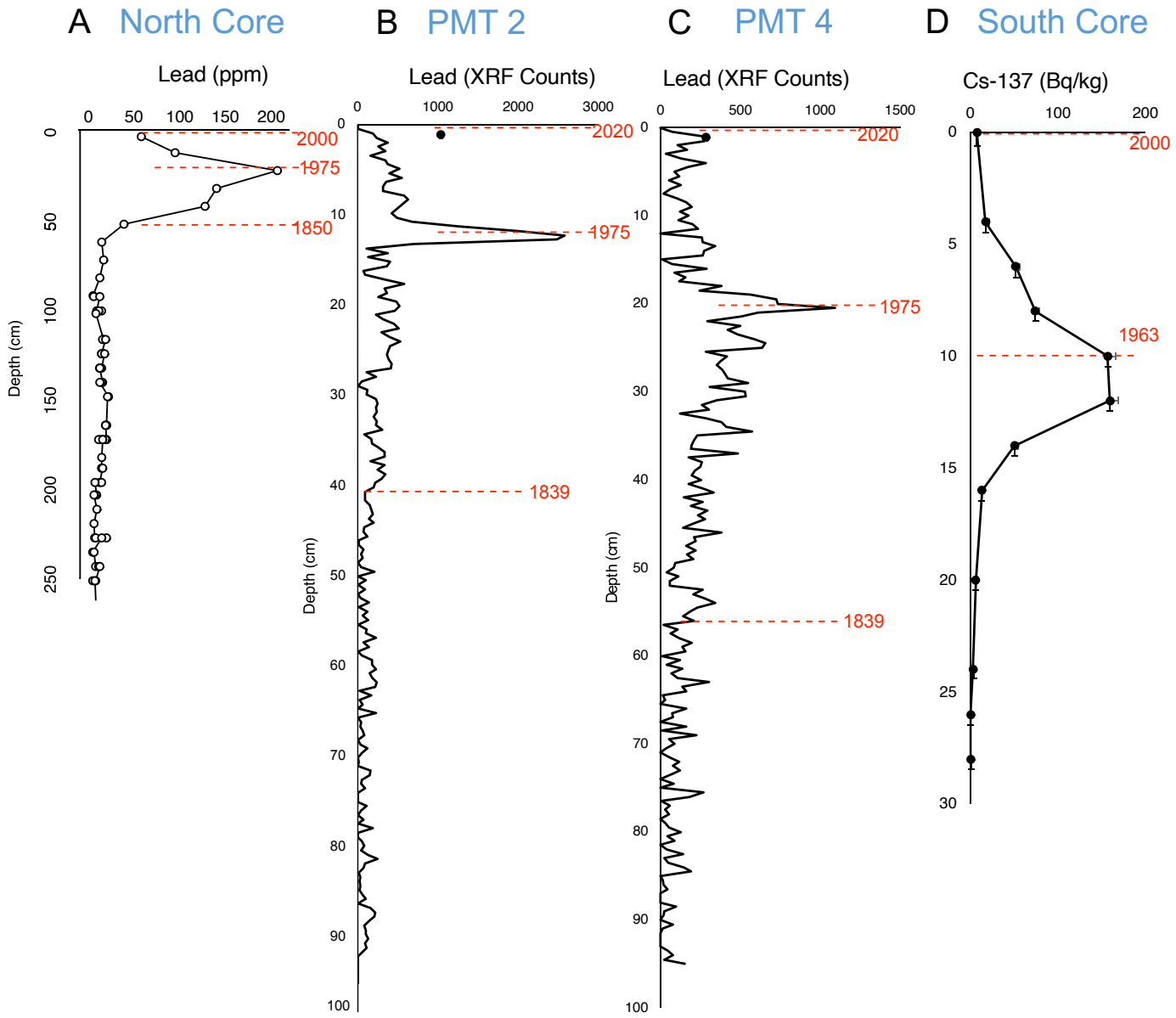

Figure 3. Lead and Cs-137 chronologies. A; Lead curve from the North Core. This data was previously published in Peteet et al. (2020). B; Lead curve from PMT 2 core. The units are in XRF counts and data was generated on the ITRAX core scanner. C; Lead curve from PMT 4 core. The units are in XRF counts and data was generated on the ITRAX core scanner. D; Cs-137 core from the South Core. The vertical error bars on the cesium-137 are sampling interval. The horizontal error bars on the cesium-137 graph are 1 sigma errors.

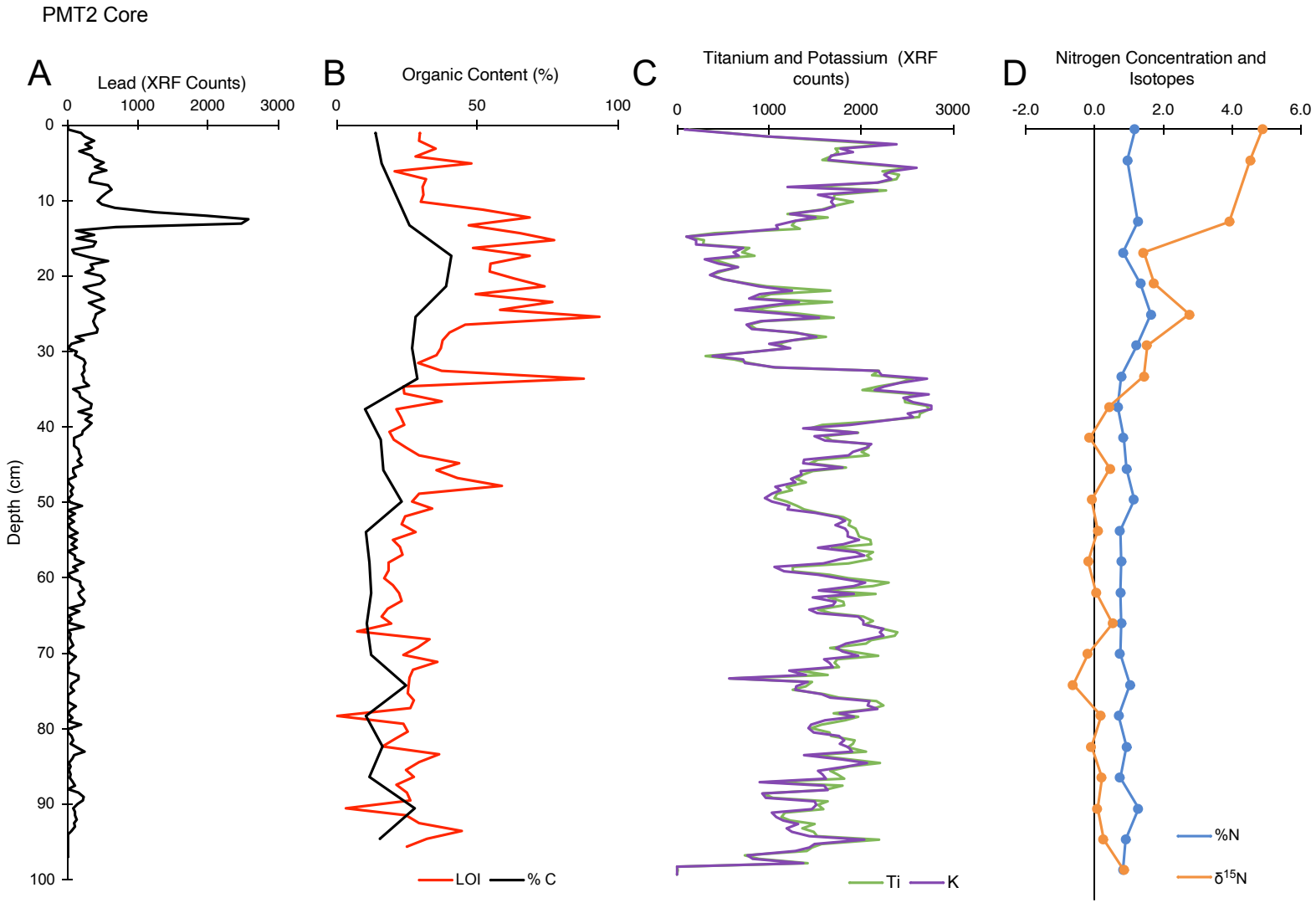

Figure 4. Down-core measurements for core PMT 2. A; lead concentration. B; % organic content measurements calculated from loss on ignition. C; titanium and potassium concentration. D; nitrogen concentration and stable isotopes. The lead, titanium, and potassium are uncalibrated XRF measurements. This decision was made because it is the down-core trend, and not the absolute value that is relevant for this study.

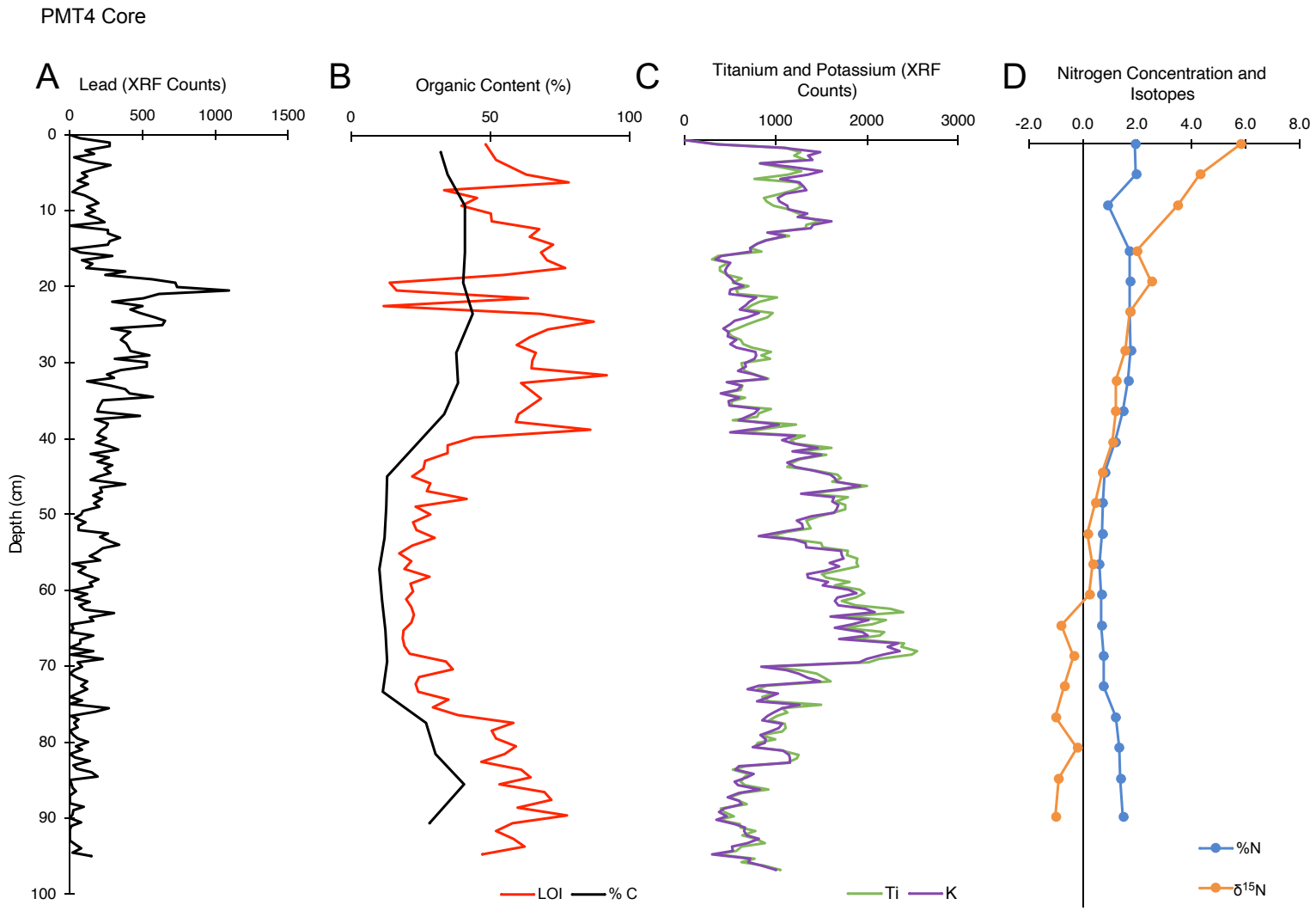

Figure 5. Down-core measurements for core PMT 4. A; lead concentration. B; % organic content measurements calculated from loss on ignition. C; titanium and potassium concentration. D; nitrogen concentration and stable isotopes. The lead, titanium, and potassium are uncalibrated XRF measurements. This decision was made because it is the down-core trend, and not the absolute value that is relevant for this study.

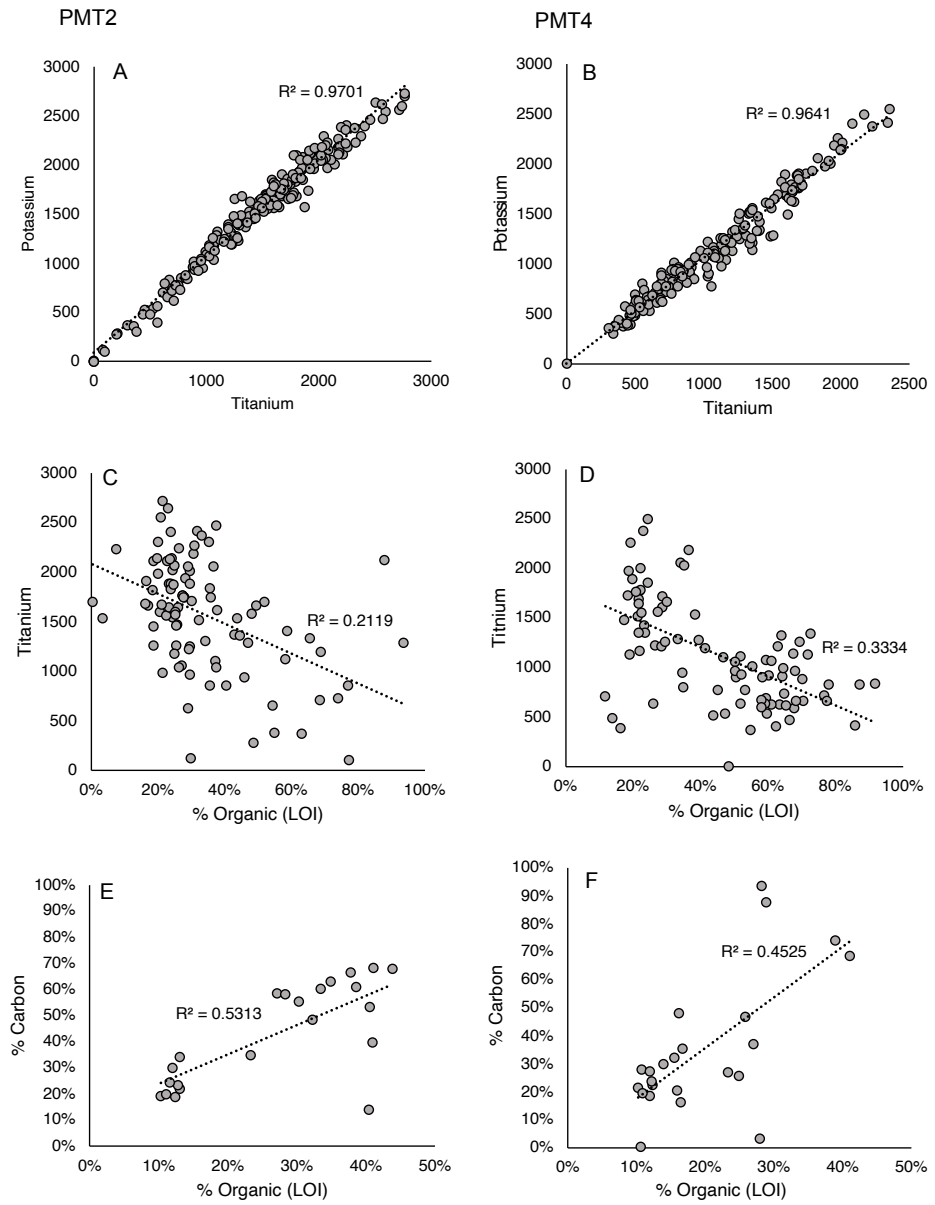

Figure 6. Relationships between potassium, titanium, LOI, and carbon. A, Potassium versus titanium for core PMT2. B, Potassium versus titanium for core PMT4. C, Titanium versus % organic content for PMT 2. D, Titanium versus % organic content for PMT 4. E, % carbon versus % organic for core PMT 2. F, % carbon versus % organic for core PMT 4.

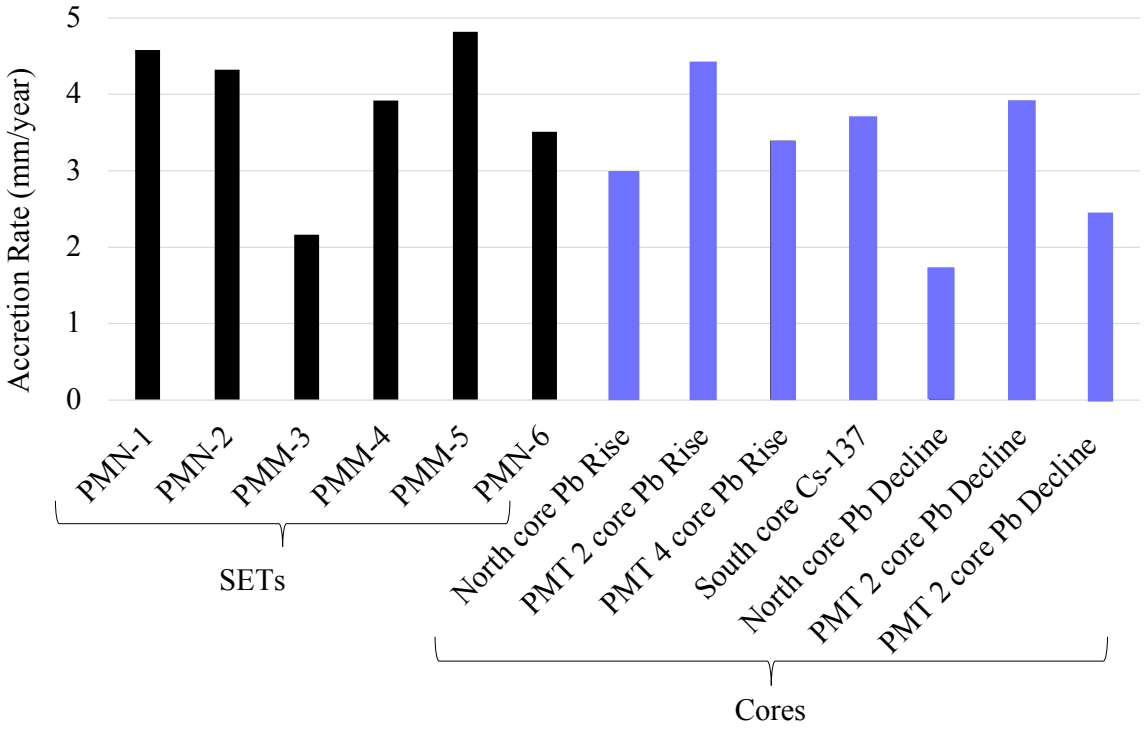

Figure 7. Summary bar chart of core and SET derived accretion rates

Table 1. RSET-MH derived accretion rates and nearby sediment cores and accretion rate calculations. [1]Roman et al., 2022; [2]Roman et al., 2007; [3]Cahoon et al., 2018; [4]Peteet et al., 2018; however, accretion rates over 350 is 2.6mm/yr; [5]Artigas et al., 2021; [6]Artigas et al., 2015; [7]Weis et al., 2021; [8]Weis et al., 2025; accretion rate is the average over the sub-estuary

Location	Average accretion rate from RSET-MH method (mm/yr)	RSET-MH monitoring duration period	Average accretion rate from core (mm/yr)	Core dating method and timescale of accretion
Fire Island, Great Gun	2.5 +/- 2	20 years (2002-2022)[1]	2.7	Pb-210, Cs-137 (44 years, 1963-2007)[2]
Fire Island, Watch Point	4.0 +/- 1	20 years (2002-2022)[1]	2.2	Pb-210, Cs-137 (44 years, 1963-2007)[2]
Fire Island, Hospital Hill	3.0 +/- 1	20 years (2002-2022)[1]	4.2	Pb-210, Cs-137 (44 years, 1963-2007)[2]
Jamaica Bay, JoCo High marsh	4.7	14 years (2002-2016)[3]	5.0	Pollution markers, pollen, radiocarbon, charcoal; (150 years; 1850-2000)[4]
Meadowlands, Secaucus High School Marshlands Site	5.52 +/- 2.15	11 years (2008-2019)[5]	1.6	Cs-137 (49 years; 1963-2012)[6]
Meadowlands, Eight Day Swamp	6.45	11 years (2008-2019)[7]	3.3	Cs-137 (1963-2002)[8]

Table 2. X-Ray Fluorescence Spectroscopy (XRF) data from core PMT 4. Data was generated on an ITRAX core scanner at the Lamont Doherty Earth Observatory Core Repository. Units are in XRF counts.

Top Depth (cm)	K	Ti	Pb
0	0	5	0
0.5	350	381	73
1	1083	1107	273
1.5	1490	1273	272

2	1353	1206	105
2.5	1401	1327	166
3	830	826	30
3.5	1162	1035	126
4	1509	1282	282
4.5	1356	1133	168
5	1053	769	85
5.5	1258	1243	118
6	1307	1278	53
6.5	1331	1197	127
7	1106	1056	64
7.5	1027	872	16
8	1038	895	102
8.5	1130	972	162
9	1133	1135	196
9.5	1348	1254	120
10	1241	1318	173
10.5	1611	1488	109
11	1410	1339	199
11.5	1384	1326	235
12	909	960	0
12.5	1094	1149	260
13	902	885	262

13.5	791	793	343
14	722	719	273
14.5	730	842	264
15	411	371	10
15.5	340	301	70
16	498	484	289
16.5	468	389	84
17	447	386	156
17.5	465	475	115
18	513	624	382
18.5	545	534	241
19	642	705	561
19.5	505	566	723
20	493	585	735
20.5	781	1011	1090
21	708	827	609
21.5	672	742	505
22	603	661	290
22.5	818	961	499
23	693	912	417
23.5	551	796	483
24	498	690	584
24.5	425	576	655

25	484	469	633
25.5	476	522	283
26	565	616	416
26.5	504	639	374
27	567	735	353
27.5	774	949	387
28	785	838	403
28.5	763	934	417
29	664	624	546
29.5	674	631	307
30	588	660	526
30.5	757	771	531
31	895	914	352
31.5	460	479	257
32	621	630	303
32.5	575	616	121
33	398	413	282
33.5	592	662	380
34	481	516	409
34.5	496	511	571
35	816	945	228
35.5	771	814	209
36	685	798	196

36.5	601	530	190
37	1031	1220	481
37.5	840	934	173
38	505	631	259
38.5	1207	1313	250
39	1069	1161	215
39.5	1192	1207	193
40	1455	1606	251
40.5	1179	1242	176
41	1493	1557	267
41.5	1242	1269	332
42	1130	1188	145
42.5	1210	1122	265
43	1404	1421	189
43.5	1601	1677	293
44	1646	1713	235
44.5	1662	1620	279
45	1922	2002	197
45.5	1695	1752	142
46	1280	1347	379
46.5	1641	1786	208
47	1621	1655	218
47.5	1688	1760	162

48	1667	1765	217
48.5	1640	1625	166
49	1391	1475	203
49.5	1229	1339	89
50	1290	1351	80
50.5	1300	1381	37
51	1074	1130	110
51.5	812	948	57
52	1199	1206	58
52.5	1327	1495	261
53	1336	1513	206
53.5	1712	1785	271
54	1719	1781	339
54.5	1744	1895	228
55	1592	1887	186
55.5	1694	1900	139
56	1543	1685	207
56.5	1344	1504	18
57	1351	1551	107
57.5	1568	1812	60
58	1515	1644	116
58.5	1795	1924	195
59	1888	1970	137

59.5	1680	1876	153
60	1649	1720	10
60.5	1686	1877	121
61	1980	2256	35
61.5	2083	2399	137
62	1596	1759	65
62.5	2013	2204	104
63	1832	2053	300
63.5	1648	1733	137
64	1953	2183	160
64.5	2004	2141	13
65	1695	1847	27
65.5	2340	2402	0
66	2227	2372	159
66.5	2356	2542	72
67	2173	2489	74
67.5	2000	2133	0
68	1911	2021	162
68.5	847	920	9
69	1120	1255	224
69.5	1254	1444	54
70	1355	1535	84
70.5	1482	1596	33

71	818	899	0
71.5	693	804	52
72	1025	961	118
72.5	929	848	78
73	792	929	119
73.5	1261	1499	66
74	1067	1072	0
74.5	978	1128	81
75	905	1011	0
75.5	850	924	267
76	1072	1096	178
76.5	1031	1107	5
77	935	1065	57
77.5	835	829	29
78	888	994	53
78.5	879	808	0
79	745	770	26
79.5	1083	1066	53
80	1142	1254	127
80.5	1155	1234	44
81	1154	1125	86
81.5	597	672	0
82	558	531	37

82.5	761	703	138
83	681	657	24
83.5	552	612	49
84	587	667	146
84.5	828	919	188
85	594	633	0
85.5	472	496	15
86	595	593	19
86.5	622	679	40
87	437	401	0
87.5	379	439	0
88	468	536	0
88.5	353	369	94
89	546	607	23
89.5	658	613	17
90	657	772	0
90.5	684	636	75
91	812	773	15
91.5	689	880	0
92	524	625	0
92.5	529	566	0
93	306	354	0
93.5	724	771	44

94	696	621	76
94.5	840	875	21
95	1001	1052	151

Table 3. X-Ray Fluorescence Spectroscopy (XRF) data from core PMT 4. Data was generated on an ITRAX core scanner at the Lamont Doherty Earth Observatory Core Repository. Units are in XRF counts.

Top Depth (cm)	K	Ti	Pb
0	85	124	0
0.5	524	541	0
1	974	961	189
1.5	1803	1686	236
2	2379	2298	377
2.5	1781	1724	253
3	1906	1746	346
3.5	1672	1692	164
4	1648	1582	344
4.5	2075	1973	373
5	2598	2548	518
5.5	2329	2232	391
6	2249	2415	546

6.5	2324	2387	351
7	2178	2185	315
7.5	1201	1405	321
8	2174	2268	579
8.5	1527	1711	631
9	1703	1702	556
9.5	1676	1909	489
10	1711	1695	428
10.5	1600	1573	493
11	1228	1196	679
11.5	1498	1636	1251
12	1272	1281	1983
12.5	1080	1242	2574
13	1098	1329	2480
13.5	570	402	692
14	98	101	113
14.5	209	291	373
15	203	279	129
15.5	719	786	406
16	615	705	364
16.5	673	837	69
17	300	376	97
17.5	450	534	327

18	655	657	579
18.5	438	483	332
19	356	368	362
19.5	503	484	256
20	699	723	479
20.5	885	969	525
21	1251	1661	464
21.5	893	1022	226
22	780	853	316
22.5	1320	1685	453
23	998	1121	509
23.5	635	804	299
24	1096	1288	399
24.5	1541	1697	528
25	901	938	403
25.5	753	779	386
26	815	857	362
26.5	1286	1236	388
27	1509	1617	422
27.5	1249	1249	414
28	1000	1098	111
28.5	1224	1201	227
29	835	850	52

29.5	382	310	0
30	715	626	123
30.5	732	786	107
31	1065	1040	229
31.5	2188	2194	249
32	2219	2115	224
32.5	2714	2567	243
33	2411	2404	202
33.5	2253	2186	234
34	2142	2013	227
34.5	2738	2608	309
35	2458	2467	79
35.5	2568	2479	170
36	2766	2710	182
36.5	2765	2739	253
37	2510	2641	335
37.5	2567	2629	331
38	2186	2138	156
38.5	1880	1574	340
39	1373	1450	251
39.5	1956	1971	344
40	1489	1595	294
40.5	1608	1680	218

41	2110	2064	204
41.5	2066	2077	89
42	1908	2005	97
42.5	1861	2083	96
43	1384	1530	149
43.5	1374	1447	170
44	1797	1834	185
44.5	1340	1476	141
45	1352	1370	204
45.5	1234	1290	80
46	1286	1400	76
46.5	1069	1191	119
47	1121	1248	10
47.5	1031	1082	19
48	955	1053	76
48.5	1031	1193	40
49	1222	1301	65
49.5	1195	1375	0
50	1502	1540	45
50.5	1749	1807	206
51	1825	1881	0
51.5	1724	1863	99
52	1825	1938	0

52.5	1850	1956	93
53	1855	1977	0
53.5	1973	2096	36
54	1806	2106	144
54.5	1533	1685	19
55	1935	2129	124
55.5	2036	2062	60
56	1778	2106	127
56.5	1584	1859	0
57	1058	1259	109
57.5	1165	1252	98
58	1530	1656	227
58.5	1761	1860	74
59	2047	2297	139
59.5	1923	2127	0
60	1544	1561	53
60.5	1919	2156	181
61	1470	1645	182
61.5	1724	1808	230
62	1693	1817	150
62.5	1438	1534	176
63	1526	1675	241
63.5	1963	2025	219

64	2020	2132	28
64.5	2020	2046	169
65	2244	2230	23
65.5	2202	2391	60
66	2238	2369	0
66.5	2020	2105	227
67	1838	2055	0
67.5	1730	1664	45
68	1799	1881	29
68.5	1968	2180	60
69	1601	1740	83
69.5	1658	1711	0
70	1690	1757	29
70.5	1221	1318	122
71	1395	1638	51
71.5	569	572	0
72	1418	1468	19
72.5	1294	1394	0
73	1281	1260	156
73.5	1573	1600	153
74	1665	1759	51
74.5	2086	2162	44
75	2075	2238	95

75.5	2178	2116	0
76	1770	1700	0
76.5	1922	1965	0
77	1603	1826	116
77.5	1459	1572	44
78	1427	1459	0
78.5	1485	1657	69
79	1758	1670	0
79.5	1817	1931	189
80	1771	1908	0
80.5	1863	1855	7
81	1902	2055	57
81.5	1381	1487	82
82	1798	1877	47
82.5	2061	2207	130
83	1842	1871	244
83.5	1529	1660	91
84	1581	1739	71
84.5	1617	1813	14
85	897	978	37
85.5	1598	1795	22
86	1636	1599	38
86.5	927	934	27

87	959	1035	66
87.5	1495	1633	100
88	1513	1535	0
88.5	1462	1588	158
89	1024	1173	223
89.5	1073	1132	212
90	1154	1224	145
90.5	1311	1492	81
91	1194	1357	105
91.5	1246	1485	104
92	1432	1517	135
92.5	2032	2191	92
93	1494	1570	107
93.5	1437	1465	58
94	1280	1408	0
94.5	768	733	0
95	818	887	0
95.5	1371	1419	0
96	0	0	0
96.5	0	9	0
97	0	0	0

Table 4. Loss on Ignition (LOI) data from core PMT 2. The units are in percent (%) lost after 4 hours of combustion at 550°C.

Interval	LOI
0-2	48%
2-4	52%
4-5	63%
5-6	78%
6-7	33%
7-8	45%
8-9	40%
9-10	50%
10-11	50%
11-12	67%
12-13	64%
13-14	73%
14-15	68%
15-16	70%
16-17	77%
17-18	55%
18-19	14%
19-20	16%
20-21	63%
21-22	12%
22-23	68%

23-24	87%
24-25	71%
25-26	64%
26-27	59%
27-28	66%
28-29	65%
29-30	65%
30-31	92%
31-32	61%
33-34	68%
35-36	60%
36-37	59%
37-38	86%
38-39	44%
39-40	35%
40-41	35%
41-42	26%
42-43	26%
43-44	22%
44-45	29%
45-46	27%
46-47	41%
47-48	23%

48-49	29%
49-50	22%
50-51	24%
51-52	30%
52-53	22%
53-54	17%
54-55	22%
55-56	19%
56-57	28%
57-58	21%
58-59	22%
59-60	20%
60-61	22%
61-62	23%
62-63	22%
63-64	19%
64-65	19%
65-66	19%
66-67	21%
67-68	34%
68-69	37%
69-70	24%
70-71	23%

71-72	24%
72-73	35%
73-74	29%
74-75	38%
75-76	58%
-76-77	50%
77-78	52%
78-79	59%
79-80	55%
80-81	47%
81-82	61%
82-83	65%
83-84	53%
84-85	69%
85-86	72%
86-87	60%
87-88	78%
88-89	58%
89-90	52%
90-91	58%
91-92	62%
92-93	47%

Table 5. Loss on Ignition (LOI) data from core PMT 4. The units are in percent (%) lost after 4 hours of combustion at 550°C.

Interval	LOI
0-1	30%
1-2	29%
2-3	35%
3-4	28%
4-5	48%
5-6	21%
6-7	32%
7-8	31%
8-9	31%
9-10	30%
10-11	52%
11-12	69%
12-13	47%
13-14	65%
14-15	77%
15-16	49%
16-17	69%
17-18	55%
18-19	54%
19-20	63%

20-21	74%
21-22	49%
22-23	77%
23-24	58%
25-26	93%
26-27	46%
27-28	40%
28-29	38%
29-30	37%
30-31	35%
31-32	29%
32-33	37%
33-34	88%
34-35	24%
35-36	24%
36-37	37%
37-38	21%
38-39	23%
39-40	24%
40-41	19%
41-42	21%
42-43	25%
43-44	29%

44-45	44%
45-46	35%
46-47	43%
47-48	59%
48-49	29%
49-50	27%
50-51	34%
51-52	24%
52-53	23%
53-54	28%
54-55	20%
55-56	23%
56-57	24%
57-58	19%
58-59	19%
59-60	17%
60-61	20%
61-62	22%
62-63	23%
63-64	18%
64-65	16%
65-66	20%
66-67	7%

67-68	33%
68-69	29%
69-70	24%
70-71	36%
71-72	27%
72-73	26%
73-74	26%
74-75	25%
75-76	27%
-76-77	26%
77-78	0%
78-79	24%
79-80	25%
80-81	21%
81-82	16%
82-83	37%
83-84	30%
84-85	25%
85-86	27%
86-87	21%
87-88	25%
88-89	26%
89-90	3%

90-91	25%
91-92	29%
92-93	44%
93-94	32%
94-95	25%

Table 6. SET accretion rates from Piermont Marsh measured from May 2019 to October 2023. SET 2 is 2 m from core PMT 2. SET 4 is 2 m from core PMT 4.

Site Code	Accretion (mm/year)
SET-1	4.9
SET-2*	5.2
SET-6	4.5
SET-3	3.1
SET-4*	5.6
SET-5	6.5

Table 7. Accretion rates calculated from sediment cores. *The North sediment core is from Peteet et al. 2020.

	Years of Accretion Captured	Method	Depth of horizon	Number of years	Accretion rate (mm/year)
North core*	1840-2000	Pb-rise	54.5	161	3.0
PMT 2	1840-2020	Pb-rise	41	181	4.4
PMT 4	1840-2020	Pb-rise	56	190	3.4
South core	1963-2001	Cs-137	10	38	3.8
North core	1975-2000	Pb-decline	14.5	25	1.7
PMT 2	1975-2020	Pb-decline	11.5	45	3.9
PMT 4	1975-2020	Pb-decline	18.5	45	2.4

Table 8. δ15N and %N values at 0-1cm

Sample	**δ15N vs. At. Air (‰)**	**%N**

PMT2 2021	4.88	1.16
PMT4 2021	5.80	1.92
Piermont 2000	4.20	1.00

Offset Between Surface Elevation Table and Sediment Core Derived Accretion Rates: Case Study from Piermont Marsh, New York
Electronic Supplemental Material
March 4, 2025

Clara Chang[1*], Sarah Fernald[2], Timothy Kenna[1], Christopher Mitchell[2], Christina Pacella[2], Margie Turrin[1], Jonathan Nichols,[1] Steven Chillrud[1], Dorothy Peteet[1,3]
[1]*Lamont Doherty Earth Observatory of Columbia University, Palisades, NY, 10968, USA*
[2]*Hudson River National Estuarine Research Reserve, Staatsburg, NY, 12580*
[3]*NASA Goddard Institute for Space Studies, New York, NY 10025*
*corresponding author, Clara Chang, cchang@ldeo.columbia.edu, ORCID ID: 0000-0001-7310-639X

Table S1. Carbon and Nitrogen Concentration and Isotope Data for core PMT 4. This data was measured by the Cornell University Stable Isotope Laboratory (COIL) on a Thermo Delta V isotope ratio mass spectrometer (IRMS) interfaced to a NC2500 elemental analyzer.

Top	Bottom	Weight (mg)	%N	δ15N vs. At. Air	%C
0	2	5.09	1.9	5.8	32
4	5	4.968	2.0	4.3	35
8	9	5.006	0.9	3.5	41
14	15	5.17	1.7	2.0	41
18	19	5.102	1.7	2.5	40
22	23	5.023	1.7	1.7	44
27	28	5.085	1.7	1.5	38
31	32	4.986	1.7	1.2	38
35	36	5.014	1.5	1.2	33
39	40	4.931	1.2	1.1	23
43	44	5.114	0.8	0.7	13
47	48	5.188	0.7	0.5	13
51	52	5.181	0.7	0.2	12
55	56	5.086	0.6	0.4	10
59	60	5.1	0.7	0.2	11
63	64	5.014	0.7	-0.8	12
67	68	5.098	0.8	-0.4	13
71	72	5.079	0.7	-0.7	12
75	76	5.116	1.2	-1.0	27
79	80	5.133	1.3	-0.2	30

83	84	4.898	1.4	-0.9	40
88	89	5.007	1.5	-1.0	28

Table S2. Carbon and Nitrogen Concentration and Isotope Data for core PMT 2. This data was measured by the Cornell University Stable Isotope Laboratory (COIL) on a Thermo Delta V isotope ratio mass spectrometer (IRMS) interfaced to a NC2500 elemental analyzer.

Top	Bottom	Weight (mg)	%N	δ15N vs. At. Air	%C
0	1	5.176	1.2	4.9	14
4	5	5.141	0.9	4.5	16
12	13	5.101	1.3	3.9	26
16	17	1.917	0.8	1.4	41
20	21	5.084	1.3	1.7	39
24	25	4.998	1.6	2.8	28
28	29	5.127	1.2	1.5	27
32	33	5.064	0.8	1.4	29
36	37	4.982	0.7	0.4	10
40	41	5.011	0.8	-0.2	16
44	45	5.032	0.9	0.4	17
48	49	5.008	1.1	-0.1	23
52	53	5.205	0.7	0.1	11
56	57	5.066	0.8	-0.2	12
60	61	5.144	0.8	0.0	12
64	65	5.328	0.8	0.5	11
68	69	5.036	0.7	-0.2	12
72	73	5.127	1.0	-0.6	25
76	77	5.063	0.7	0.2	10
80	81	4.956	0.9	-0.1	16
84	85	5.113	0.7	0.2	12
88	89	4.834	1.3	0.1	28
92	93	5.047	0.9	0.3	15
96	97	5.008	0.8	0.8	16

Table S3. Cesium-137 data from core PMT S01. This core is in the south of Piermont marsh.

Upper Depth	Lower Depth	Mass (g)	Cs-137 (pCi/kg)
0	2	0.969	204

4	6	0.973	472
6	8	1.32	1396
8	10	1.85	1999
10	12	1.42	4235
12	14	1.46	4303
14	16	1.39	1360
16	18	1.39	353
20	22	1.37	169
24	26	1.58	80
26	28	1.83	2
28	30	1.89	8